Tailored functional materials as robust candidates to mitigate pesticides in aqueous matrices—a review

Tahir Rasheed [a,*], Komal Rizwan [b], Muhammad Bilal [c] Farooq Sher [d], Hafiz M.N. Iqbal [e]

[a]School of Chemistry and Chemical Engineering, Shanghai Jiao Tong University, Shanghai 200240.

[b]Department of Chemistry University of Sahiwal, Sahiwal, 57000, Pakistan.

[c]School of Life Science and Food Engineering, Huaiyin Institute of Technology, Huaian 223003, China.

[d]Department of Engineering, School of Science and Technology, Nottingham Trent University, Nottingham NG11 8NS, United Kingdom.

[e]Tecnologico de Monterrey, School of Engineering and Science, Monterrey, 64849, Mexico.

*Corresponding author emails: masil@sjtu.edu.cn (T. Rasheed).

Abstract

Pesticides are among the top-priority contaminants, which significantly contribute to environmental deterioration. Conventional techniques are not efficient enough to remove pollutants from environmental matrices. The development of functional materials has emerged as promising candidates to remove and degrade pesticides and related hazardous compounds. Furthermore, the nanohybrid materials with unique structural and functional characteristics, such as better material anchorage, mass transfer, electron-hole separation, and charged interaction make them a versatile option to treat and reduce pollutants from aqueous matrices. Herein, we present the current progress in the development of functional materials for the abatement of toxic pesticides. The physicochemical characteristics and pesticide-removal functionalities of various metallic functional materials (e.g., zirconium, zinc, titanium, tungsten, and iron), polymer, and

carbon-based materials are critically discussed with suitable examples. Finally, the industrial-scale applications of the functional materials, concluding remarks, and future directions in this important arena are given.

Keywords: Environmental pollution; Pesticides; Functional materials; Adverse impact; Mitigation

Introduction

Water is among the most indispensable constituent of various biotic ecosystems. The vulnerable and uninterrupted exploitation of water resources, off-the-cuff utilities of the human-made chemicals, and growing population have instigated the mitigation of the environment (Sahoo and Gupta, 2012). The traces of pesticides protect them from recognition and obstructs the development of an operative treatment methodology. Micropollutants such as pesticides contributed a lot to the deterioration of the environment. These toxicants are acutely dangerous even in a trace amount, e.g., simazine in μg/L in water bodies can potentially cause kidney congestion, low blood pressure, heart, adrenal gland and lung related consequences (Boruah et al., 2021). These contaminants are present in unprocessed discharge from domestic wastewater, industrial effluents, cultivated fields, wetlands, and polluting natural resources (Figure 1). The United States Environment Protection Agency (USEPA) and European Environment Agency (EEA), both have declared pesticides as priority contaminants on the bases of their harmful and persistent environmental impacts (Wade et al., 2003; Rani et al., 2017). The foreseeable harmfulness of the pesticides is because of the presence of micro compounds such as dioxins, phenols, and cyanides, etc. The toxicity of these micro compounds owes to the fact that they are resilient to the conventional treatment methodologies (Debnath and Gupta, 2018; Vaya and

Surolia, 2020; Bayantong et al., 2021; Hashimoto et al., 2021). Their hydrophobic character has facilitated the assimilation of the pesticides in fatty tissues for a more extended period. The persistence of these contaminants and their accumulation in more significant concentration outcome adverse impact on living organisms. This increased level further obstructs the normal functioning of the endocrine system by disturbing the hormones (McKinlay et al., 2008). The resistive nature of these contaminants has significantly challenged the quality of usable water resources. This urges the scientists and researchers to develop advanced technologies to meet the challenge (Pillai and Gupta, 2016). Recently, the investigations are centered around the development of cutting edge tailored functional materials such as clay composites, core-shell structure, doped metal oxides, composite heterojunctions non-metal modified oxides, metal-organic framework and metal-organic framework/carbon-based hybrid nanocomposite, etc. to overcome the deficiencies (Lin et al., 2006; Cui et al., 2018). These hybrid nanomaterials are instituting their advanced applications to remove and degrade the pesticides as they exhibit better material anchorage, mass transfer, electron–hole separation, and charged interaction.

This review presents functional materials as potential candidates to mitigate toxic pesticide contamination in wastewater. Furthermore, the work focuses on the functional materials that create a lesser amount of sludge, prevent the production of secondary pollutants, and can be reused for several operations. Additionally, the basic removal pathway, negative consequences of pesticides, and their efficient handling have been discussed in detail. The fundamental sustainable developments in the manufacturing of various metallic functional materials, carbon-based materials, and polymer-based functional materials are discussed along with their advantages, such as low-cost alternatives for managing pesticides. Finally, the industrial-scale

applications of the functional materials with future prospects and recommendations are discussed.

Categories of the pesticides

The category and chemical profile of pesticides are decided based on their structure and function. , They are categorized as bactericides, fungicides, herbicides, and insecticides, based on their action on bacteria, fungi, herbs, and insects, respectively. In contrast, the organic residues of pesticides are classified based on functionalities present in their structure. They may be categorizing as pyrethroids, organophosphorus, carbamates, and organochlorine (Konstantinou et al., 2006). The pesticides are employed aerially in the form of aerosols and sprays in household areas and agricultural lands. The aerial application of pesticides may lead to the contamination of the distant regions through transboundary movement (Aktar et al., 2009). Mainly, the unpointed discharge of the pesticides from domestic wastewater and agricultural fields is hard to observe, obstructing their control (Yadav et al., 2015).

The environmental concern of the pesticides

Widespread usage of pesticides is responsible for different adverse environmental consequences and their ultimate biological effects (Figure 2). According to the Drinking Water Directive (98/83/EC) regulation, the permissible level of a single active constituent is 0.1 mg/L and for all collectively active components, the permissible level should be 0.5 mg/L in any drinking water, which is used by the humans (Karabelas et al., 2009). The documented reports reveal that the long-time intake of insecticides is responsible for interfering with the signaling of the nervous system by hindering the sodium and potassium channels and inhibiting the cholinesterase (McKinlay et al., 2008). Strong soil adsorption and resistance to biodegradation of heptachlor epoxide made them highly toxic, and its consumption causes vomiting and nausea (Grundlingh et

al., 2011). Pyrethroids are known as endocrine disruptors, and they cause various disorders as amyotrophic lateral sclerosis, dementia, genetic diseases, and Parkinson's disease. They increase the risk of childhood cancer (Slotkin, 1999; Ishihara et al., 2003). Pesticides have accumulated property. They may reside in the body from few months to several years, so even at very low concentration (ng/ml) they are dangerous for health (Graymore et al., 2001; Yadav et al., 2015). Due to their interference with cell signaling, call shocks occur, which may cause nausea, vomiting, and muscle miscoordination (Ogut et al., 2015). Different functional moieties as amides, phosphate, phenolics, and chlorine assist the uptake of pesticides on the lipophilic membranes of lungs and kidneys responsible for irreversible adverse effects (Tomer et al., 2015). Pesticide exposure may cause reproductive diseases, congenital disabilities, cancer, malignant tumors, miscarriages, genital deformations, abnormalities in behavior stunted growth of off-springs (McKinlay et al., 2008; Tayour et al., 2019; Gutiérrez-Jara et al., 2020; Yang et al., 2020). Pesticides also affect the reproductive system of fishes and affect the egg-shells thickness of different birds (Al Hattab and Ghaly, 2012).

Functional materials to remove pesticide

Conventional methods have several limitations for removing the pesticides, which urged the scientists to develop advanced functionalized materials and subsequent processes. The functionalization of hetero-structures enhances the physical and chemical characteristics of materials. Photoactive materials exhibit enhanced efficacy because the restricted movement of electrons and the appearance of discrete energy-levels are responsible for improving the material property. The significant properties of functional materials may be due to their improved surface defects, enhanced surface-area to volume ratio, excellent mobility of electrons, greater absorption of light, and excellent affinity for metabolites sorption in aqueous form (Lin et al.,

116 2006). These materials can be easily tailored to polymers, zeolites, and membranes to assist their
117 operation with ease. Functional materials play a significant role in treating dangerous waste
118 materials, sustainable products and sensor developments, *etc*. (Mohmood et al., 2013; Qu et al.,
119 2013).
120 Modified structures are responsible for improving the physical characteristics of materials and
121 enhancing the catalytic, magnetic, adsorbing, electrical, luminescence, and filtration
122 characteristics of the material (Reddy and Kim, 2015). So far, various functional materials have
123 been tailored and established to remove pollutants and incorporate characteristics of photo-
124 catalytic oxidation. Those functional materials suitable for treating broad spectrum molecules of
125 pesticides also do not cause any pollution in aqueous media. These challenges regarding
126 functional materials urged the scientist to research non-toxic benign templates of carbon, zinc,
127 iron, titanium, tungsten, zirconium, and polymers. For instance, graphene, carbon-nanotubes,
128 different oxides of iron as magnetite and hematite, titanium dioxide (TiO_2), zirconium oxide
129 (ZrO), zinc oxide (ZnO), and tungsten oxides are found efficient in the removal and degradation
130 of pesticides from aqueous media (Khajeh et al., 2013; Al-Hamdi et al., 2016). To decrease the
131 treatment cost, different biomaterials can be used as alternatives to expensive adsorbents. Natural
132 sources may provide carbon and biomaterials, which are obtained from polymers. They provide
133 an excellent template to produce functionalized membranes. The dendrimers with functional
134 surface modified and surface plasmonic species effectively adsorb the contaminants (Adachi et
135 al., 2004). In water treatment, materials have been found actively involved in photo-catalytic
136 degradation and adsorption of organic pollutants on their porous surface (Pillai et al., 2015;
137 Reddy et al., 2016). The active sites on porous surface materials are responsible for the
138 interaction of solid-phase with pesticide. Attempts are being to fabricate functional materials

with overcome loopholes as surface-passivation, high aggregation, and high-surface energy. Tungsten, zinc, and titanium metal oxides have great potential to absorb a specific light spectrum.

Pesticide catalysis is a new methodology to mineralize pollutants by generating low amounts of by-products, usually water and carbon dioxide. Their light absorption capability aids the catalytic property of functional materials. After functionalization, the catalytic properties and photon capture capacity of catalysts are enhanced so that they can be re-used many times to treat pesticides. The light absorption depends on the photocatalyst band gap. When light energy exceeds the material band-gap, an electron-hole pair generates only (Lam et al., 2014). The transfer of charge and channeling on the surface of the catalyst is enhanced by a greater specific surface area (Zangeneh et al., 2015). Functional materials may overcome bottlenecks of photo-oxidation as plasmonic-species, metal, and non-metal complexes charge recombination by coupling photoactive materials with polymers and sensitized dye molecules. Charge-transfer within the semiconductors increases by the formation of additional discrete band-state. The plasmonic species like gold and silver decrease charge carrier recombination. Electrons are pumped into the conduction band by these species, and life time of positive holes increases in valence-band, which completes the oxidative species generation (Luo et al., 2015). The electrons generation is facilitated by dye-sensitization of photo-catalyst, which is ascribed for the process of photo-reduction. This phenomenon can enhance the efficacy of photo-catalyst by inserting electrons from the highest occupied molecular orbital (HOMO) to the CB of semiconductor through the lowest unoccupied molecular orbital (LUMO) (Albay et al., 2016; Alam et al., 2017). Figure 3 presents various tailored functional materials for the treatment of pesticides and related environmental pollutants.

Functional materials based on Titanium

The photocatalyst TiO_2 has high mobility of electrons and can quickly generate the electron-hole pair, which enhances its capacity to effectively degrade the organic contaminants (López-Ayala et al., 2015; Sivagami et al., 2016). TiO_2 has UV sensitivity, and its bap gap falls in the range of 3.2-3.4 ev (Lee and Park, 2013; Justh et al., 2017). Different titanium oxides exist in different phases as rutile, anatase, and brookite (Chitose et al., 2003; Follut and Leitner, 2007).

The charged electrons (e_{CB}^-) and holes (h_{VB}^+) are generated when the light having more energy than the band gap falls on the surface of TiO_2 as presented in Equation (1) (Chen et al., 2011).

$$TiO_2 + h\nu \longrightarrow e_{CB}^- + h_{VB}^+ \quad \text{..... (1)}$$

Superoxides and hydroxyl radicals are generated on the surface of the catalyst when material mobilizes electrons (photo excited) from the valence to the conduction band. Available chlorine and sulfur are oxidized to chloride, and the generated holes trigger sulfide radicals and this process. While energy dissipation causes hindrance to photocatalytic efficacy, this occurs due to quick recombination of charge carriers and less visible light capability (Gupta et al., 2006; Sahoo and Gupta, 2013). Different hybrids of titanium oxides with enhanced efficiency in the visible light spectrum have been synthesized. Mainly functionalization comprises impregnating TiO_2 to the mesoporous materials like graphene, glass surface, clays, polymeric molecules, and carbon nanotubes etc. The materials strive to minimize the electron-hole pair recombination and generate additional band state, which helps absorb the visible light (Linsebigler et al., 1995; Lee et al., 2015; Cho et al. By using $AgCl/Ag/TiO_2$ (silver chloride/ silver/titanium oxide) a sandwiched type structure has been reported which enhanced the capability of TiO_2 to absorb in the visible range (Figure 4) (Tian et al., 2014).

Silver (Ag) and gold (Au) have plasmonic properties and can pump the electrons into the conduction band of TiO_2. because of this, they are of great interest for the development of photocatalyst with enhanced qualities. The electron flow is induced by silver (Ag) surface, and silver chloride (negative surface) increased the radicals (active chlorides) generation and entrapment of holes (Wang et al., 2012; Dong et al., 2013). Simple TiO_2 nanoparticles have 5% less efficiency to degrade pentachlorophenol under visible light irradiation compared to Ag/TiO2 hybrid nanoparticles, which can degrade 80% pentachlorophenol (Zhang et al., 2012). Modified TiO_2 with metals like gold, copper, palladium, and zirconium showed enhanced formation of p-n hetero-junction and interfacial transfer of charge at the solid-liquid interface (Lee and Jang, 2014; Hernández-Gordillo and González, 2015; Naraginti et al., 2015). Yu et al. (2010) reported that gold coupling provides improved photo-electrons' localization and prohibits recombination loss. As compared to TiO_2, the metals favor the generation of holes and are responsible for promoting oxidation. Dopped material replaced the base atoms, so the modified doped TiO_2 has many surface defects, and these defects increase the separation of charges responsible for entrapping the lighter energy. The *n*-type semiconductors are converted to the *p*-type when doping is done with non-metals and this increase the sensitivity of visible-light (Zangeneh et al., 2015). Interfacial surface tension on the TiO_2 surface caused by the metal impregnation increase the mesoporous surface area. This also enhances the transfer of the electrons from the metal conduction band to the TiO2 surface, reducing the divalent oxygen to the superoxide (Hossaini et al., 2014; Sahoo and Gupta, 2015). In the absorption spectrum of TiO_2, the activity of visible light is monitored by red shift, which increases the apparent quantum-yield (Linsebigler et al., 1995). TiO_2 has been modified with Cetyl Trimethyl Ammonium Bromide (CTAB) surfactant to enhance the stability of the photo-excited species and also to give the best anchorage for the

interaction of solid-liquid phase with organic compounds (Zhu et al., 2007). Increased removal and degradation of the pesticides may be due to the co-adsorptive capability of surfactant-bilayer (Senthilnathan and Philip, 2010). Enhanced dispersion of particles was also provided by surfactants which give a homogeneous surface for the degradation and adsorption of metabolites. Modification of TiO_2 particles with iron particles or silica beads has been carried out to better separate TiO_2 particles from aqueous phase both magnetically and physically. Organo-phosphorus based pesticides have been degraded by the immobilization of TiO_2 on silica beads (Shifu and Gengyu, 2005). Liu and his co-workers synthesized the Fe/TiO_2 nano-particles for the degradation of 2,4-dinitrophenol (Liu et al., 2012).

Fe_2O_3/TiO_2 has been employed for 2,4-dichlorophenoxyacetic acid degradation (Figure 5) (Lee et al., 2017). Photogenerated electrons get excited from the valence band to the conduction band of TiO_2 after exposure of photocatalyst to UV light, and holes left are left in the valence band. 2,4-dichlorophenoxyacetic acid oxidized directly to 2,4-dichlorophenol through these photogenerated holes. Reduction of oxygen takes place because holes and superoxide radicals are generated. Heteroconjuction formation between Fe_2O_3 and TiO_2 nanoparticles led to the promotion of charge transfer, which also suppressed the electron-hole recombination. Table 1 presents the efficiency of different titanium-based materials for the degradation and removal of different pesticides

Functional materials based on Zinc

Zinc-based materials with novel crystalline and characteristics have been developed with efficient photo-catalytic properties. These materials have the property of reusability for many degradation processes. Low toxicity, economic values, less light scattering, easy tailored-surface characteristics, and good mobility of E-H pair made zinc the best option for pesticide

degradation. The inhibition of recombination of E-H pair, quantum entrapment, and loss of heat energy are the main factors responsible for the efficacy of photocatalysis (Shanmugam and Jeyaperumal, 2018). The Refractive index of ZnO is 2, and it has a band gap of 3.2 eV. It has an efficiency of maximum light absorption. As compared to TiO_2, ZnO produces more reductive species due to the excellent mobility of electrons, and similarly, the oxidative potential of hydroxyl radicals is higher in ZnO (3.0 V) in comparison to TiO_2 (2.7 V) (Kumar and Rao, 2015). Despite being a promising photocatalyst, ZnO also has potent antimicrobial properties (Navarro et al., 2009; Bechambi et al., 2015). Photo-corrosion, photo dissolution, fast E-H pair recombination, and also at alkaline pH, the creation of the surface-passive-layer ($Zn(OH)_n^{(2-n)+}$) are the limitations of ZnO, which decreases its efficacy and versatility (Panthi et al., 2015). Equation (2) presents the reaction process (Kumar and Rao, 2015) where 'n' is dependent on the solution pH. Initially, the ZnO photo dissolution involves the hole trapping (h^+) on the surface, resultantly oxygen molecules are generated (O_2), and then the creation of the surface-passive-layer ($Zn(OH)_n^{(2-n)+}$) happens.

$$ZnO + 2h^+ + nH_2O \longrightarrow Zn(OH)_n^{(2-n)+} + 1/2\ O_2 + nH^+ \quad \text{..... (2)}$$

By incorporating carbon-nanotubes, polymers, metals, non-metals, and surfactants, researchers have developed modified ZnO materials to overcome these limitations. These modifications can inhibit Photo-corrosion and the formation of the passive layer. Divband et al. (2013) presented the importance of the fermi-level for the potential transfer of the electrons from the conduction-band of ZnO to silver, which consequently entraps the oxygen and forms the super-oxides. ZnO complexes with HCA (hydrocitric acid)/TBPA (tetra-bromophthalic anhydride) increased the visible-light sensitivity of ZnO (Comparelli et al., 2005). Complexation of ZnO with chitosan to degrade the permethrin (pesticide) has been reported (Dehaghi et al., 2014). The polymer-zinc

oxide composite at the dose of 0.5 g/L degraded the 99% pesticide. After 3 cycles, the composite showed 56% efficacy. Coating the polymer on ZnO gives strength to functional material against the photocorrosion, and also polymer may also act as an electron-pumping agent. Pei and co-workers (Pei et al., 2014) described the increased photocatalytic efficacy of coupled ZnO with poly-aniline. And this attributed the process to the excellent capture of the electrons. Dyes and polymers have mobile charge carrier potential and may help in the easy transfer of electrons. In the acidic media, the polymers protonate conveniently, which protects ZnO's dissolution in acidic media and helps efficient binding of negative charge containing organic contaminants (Khatamian et al., (2012). In the continuous-flow reactor, the composite of ZnO-bentonite having an approximate size of 20-30 nm degraded the phenol (70%) with an adsorption potential of 14.7 mg/g (Meshram et al., 2011). Bentonite clay has many layers of silicate and aluminum hydroxide, which probably responsible for the removal mechanism. They have excellent absorbing power and enhance the surface area of the catalyst, which is attributed to improving the solid-liquid mass transfer operations. ZnO has been hybridized with rare earth metals as nobelium and lanthanum to control the E-H pair recombination (Anandan et al., 2007a; Anandan et al., 2007b; Lam et al., 2014). Doping of lanthanum in ZnO enhanced the space charge potential more than 0.2 V which gave the effective E-H pair separation (Anandan et al., 2007a). ZnO modified with ferric oxide provided enhanced surface-area and also showed enhanced absorption of visible light to efficiently degrade the penta-chlorophenol (Xie et al., 2015). Fast diffusional metabolites transfer occurs to the mesoporous structure (flower like) which then reacts with radicals.

The ZnO has been coupled with silver to efficiently remove the phosphamidon (an organo-phosphorus pesticide) (Korake et al., 2012). Catalyst at conc. of 1 g/dm^3 (at pH = 7) degraded the

phosphamidon (at initial conc. of $5x10^{-2}$ mol/L) within 150 minutes. Widespread use of ZnO is hindered because of low quantum yield due to out-ward electron diffusion. To prevent the recombination and entrapment of holes, the formation of p-n hetero-junction is an efficient method (Pirhashemi and Habibi-Yangjeh, 2017). Improvement in visible-light activity of ZnO has been made by grapheme, which potentially enhances the shelf-life of radicals and provides a larger surface area for pesticide interaction (Darwish et al., 2017). The doping of nitrogen and silver obtained the modulation in the ZnO bandgap in the ZnO lattice (Debnath and Gupta, 2018). And this tailored functional material increased the degradation of 2,4-di-nitrophenol (2,4-DNPH). Co-doing with metal and non-metal and decrease in the band gap helped generate the bulk attributed to enhancing the photo-catalytic potential of ZnO by absorption of the wide light spectrum and low dissipation of heat. Role of different Zinc based functional materials for degradation and removal of pesticides has been presented in Table 1.

Functional materials based on Tungsten

Ultra-violet (UV) active photocatalysts cannot absorb in the visible light region, which is a significant part of the solar light spectrum. While many semiconductors have wider band-gaps which UV light energy activates only. Tungsten oxides have a narrow band-gap (2.3-2.5 eV), activated in visible light energy. The tungsten trioxide (WO_3) complexes with different materials or semi-conductors are under consideration to explore its photo-catalytic potential. The WO_3 was found in mono-clinic I and mono-clinic II phases (Tahir et al., 2017). Recombination, dissipation of absorbed energy, and generation of E-H pairs are processes that decrease the efficacy of WO_3 due to its small bandgap. Mesoporous WO_3-TiO_2 degraded the imazapyr, phenolics, and malathion with efficient removal greater than 100, 98, and 76%, respectively (Aslam et al., 2014; Ismail et al., 2016). The mechanism may be due to less light scattering and increased diffusion of

organic motifs in catalyst surface (porous). Convenient transfer of oxidative holes from WO_3 to TiO_2 produces radicals that increase the oxidation. Surface impregnation with Pd (palladium) metal enhanced the surface response of WO_3 (Mkhalid, 2016). Graphite electrodes have been coated with WO_3 for efficiently removing the 2-nitrophenol around 82%. Figure 6 showed the mechanism of the photo-assisted activity of the WO_3-EG composite electrode for the degradation of 2-nitrophenol. (Umukoro et al., 2017). Table 1 presents the efficiency of different tungsten-based materials for the degradation and removal of different pesticides

Functional materials based on Iron

Iron has a mesoporous surface and exists in different forms in the earth's crust. It has both reductive and oxidative properties. Iron-based nano-materials have a surface area of 82 m^2 g^{-1} and a band gap of 2.2 eV (Pei et al., 2014). Iron-based materials are adequate for water treatment as they are easy to separate from aqueous solutions because of their magnetic characteristics. Complexes of iron as Fe/Pd, Fe/Ni transformed the chlorinated pesticides, PCBs (polychlorinated-biphenyls), HCH (hexa-chlorocyclohexane), and hydrocarbons by de-chlorination process (Cao et al., 2005; Elliott et al., 2009). Iron materials get agglomerated in aqueous media, leading to less dispersion and low surface contact with the pesticides. The incorporation of metals (Pd, Ni, Pt, and Zn) may counter the agglomeration by promoting association and dissociation of H_2 gas into the atomic hydrogen, which inhibits the oxide layers formation on iron (Tee et al., 2009). Table 1 presents the efficiency of different modified iron-based materials for the degradation and removal of various pesticides. Copper-maghemite mineralized the 4-nitrophenol efficiently (Feng et al., 2013). Zero-valent iron in nano form has significant reducing characteristics and good surface area, resulting in agglomeration, but metals and organic stabilizer compounds can stabilize it (Ayad et al., 2017). The reduction of organic

molecules may release the active radicals (bromide, sulfate, and chloride), and these radicals may indirectly oxidize the pesticides. The metal nano-particles adorned on the surface of iron oxide as Ni/Fe-Fe_3O_4 dechlorinated the di-chlorophenol within 3 hours (Xu et al., 2016a). Pesticides are mostly hydrophobic and adhere to the porous surface of the iron. Impregnation of iron oxide with either gold or silver plasmonic-species increased the *p*-nitrophenol reduction (Jiang et al., 2015). The coordination of adsorption and reduction was effective at the surface of Ag/Fe_2O_3. The electrons transfer from silver (Ag) to iron (Fe) formed the depletion-layer at the interface of Ag/Fe_2O_3 enhanced the fast organic species reduction (Chiou et al., 2013). Iron-based materials have significant porosity and permeability, which may be responsible for the potent diffusion of metabolites. The transfer of mass between the solid-liquid phase offers enough time for effective degradation. Magnetic-silica nanoparticles modified with palladium effectively degrade and remove the DDT (Tian et al., 2015). In this process, electron-channeling from the Pd-donor followed by adsorption of magnetic particles. The presentation of the Core-shell structure has been provided in Figure 7. Bimetallic iron-palladium (Fe-Pd) nano effectively degraded the lindane at an initial conc. of 5 mg/L (Tian et al., 2015). The iron-palladium (Fe-Pd) potential is attributed to the fast de-hydrohalogenation of C-Cl bond in lindane (Joo and Zhao, 2008). The amount of palladium is effective for inhibiting the agglomeration of iron (Xu et al., 2005). The coupling of magnetic particles with polymers (*e.g.*, starch) and surfactants (*e.g.*, CTAB) provided excellent coherence of contaminated materials (Zhao et al., 2008; Gao et al., 2013). Magnetic particles coated with the starch effectively reduced the 98% of tri-chloroethylene (TCE) in the period of 1 hour (He and Zhao, 2005). Zeta-potential played a role in glyphosate removal by the $MnFe_2O_4$-graphene-nanomaterial (Yamaguchi et al., 2016). Incorporation of Fe_2O_3 on the carbon nano-tubes enhanced the surface area which increased the atrazine (pesticide) removal within

120 minutes using H_2O_2 (Yu et al., 2015). Fast de-alkylation, alkylic-oxidation and de-chlorination and available adsorption sites on the carbon-nanotubes attributed to the removal of the pesticide (Graymore et al., 2001). Iron-based materials are reported to degrade nitro-aromatic pesticides which may convert the anilines to respective amine or various other nitroso compounds (Keum and Li, 2004).

Functional materials based on Carbon

A primal element, carbon, formulae the fundamental construction unit of life expectancy. In water treatment, the actuated carbon material is extensively used as an adsorbent. The nanoscale dimension and the adaptable characteristics of carbon are significantly improved, such as high thermal and mechanical properties, improved electrical conduction, etc. Various carbon-based materials, including carbon quantum dots, g-C3N4, carbon nanotubes, and graphene, are available as various nanomaterials based on their architectural properties. Such materials have a high volume to surface area and a particularly closer band gap (Yue and Economy, 2005). Carbon is hydrophobic and has a great affinity for non-polar phenols and pesticides. On the other hand, because of the absence of chemical activity, graphene and carbon nanotubes take a long time to adsorb organic pollutants. Conventionally, to ensure the cost-effective removal of pesticides from water, carbon-based activated materials with its increased characters of improved porosity and surface area have been investigated. Besides, carbon materials demonstrate considerable high-temperature stability, making the expended adsorbent readily available after adsorption. The production of carbon-based activated materials from waste tyres and rubber and its successive usage for atrazine, methyl parathion, and methoxychlor extraction were stated by Gupta and co-workers (Gupta et al., 2011). Carbonaceous materials based on hydrogen bonds, π-π interactions, porous nature of the surface, and covalent bonds, making it an excellent

hydrophobic contaminant removal substrate. Biomaterials can sometimes be fabricated by carbon-based materials that afford cheaper alternatives to treat pesticides, such as banana peel, rice husk, olive stone, coconut shell, eggshell, etc. The oil seed matrix as an innovative material for the collaborative elimination of hydrophobic pollutants based on the water/octanol partition coefficient has been examined for this purpose (Boucher et al., 2007). The successful elimination of chlorpyrifos DDE and endosulfan owes because of reduction in compounds by halogen group oxidation accompanied by adsorption on RGO exfoliated sheets by π-π graphene surface interactions. (Yue and Economy, 2005; Cho et al., 2018). Previous studies have also examined the successful removal of nitrophenols, pesticides, and chlorobenzene from carbon nanotubes (Peng et al., 2003; Cai et al., 2005). Based on structure, the carbon nanotubes are normally multi-walled or single-walled. In developing solid-phase extraction systems, the flexible properties of nanotubes have also been used. Even at low concentrations (4-13 ng/L), pesticides, such as sulphonyl urea and DDT, have been eliminated. This elimination owes to the extraordinary, which can be due to the unusual attraction of CNTs with functionalities present in the structure of pesticide (Zhou et al., 2006). It is worth mentioning here that the sheet purity, degree of twist, diameter of the tube, geometric character, physical/chemical character, and the synthetic method ascertain remarkable properties to the CNTs (Debnath et al., 2019). The polar and nonpolar bonds present in different molecules (COOH, NH_2, C-C, C-O) interact with these π-π interactions (Pan and Xing, 2008). Therefore, the symbiotic structure of adsorbing catalysis can effectively eliminate pesticides, and designing such functional materials is imperative. Carbon-based particles can be very easily modified by cationic and anionic surfactants on the surface. This modification leads to ionic modulation of the carbon-based surface, which can easily interact with the oppositely charged surface of pesticide (Park and Bae, 2015). Wang and

Coworkers documented MWCNT conjugated TiO_2 based material to mitigate dinitrophenol (Wang et al., 2009). Shi et al. documented the CNT-based materials conjugated with Ag/AgCl through the ultrasonication-based deposition-precipitation method to remove tribromophenol (Shi et al., 2013). The new materials resolve the issues related to the low reactivity of CNTs against intransigent carbon assisted compounds by plasmon action of silver. Electrons are injected by plasmon into the silver bromide conduction band, whose conduction band is more negative than silver (0.065 V vs. 0.2 V). Moreover, the electrons guide the flow to the mobile surface of CNTs. Often, silver-based compounds can enhance the activity of visible light. Compounds such as Ag_2S with a 0.9-1.05 eV band gap have been stated to cause the reaction under visible light reaction (Huo et al., 2018). Recently, to catalyze the degradation of 4-nitrophenol, g-C_3N_4 coupled with nickel has been effectively synthesized. In this degradation process the impregnated Ni is the major cause of degradation process as it donates electron and enhances the effectiveness of the process. This matrix (g-C_3N_4-Ni) contains highly oxidative holes which can enhance the degradation mechanism. The improved character of Pd-mesoporous carbon based materials engineered by irradiation for the degradation of nitrophenol has also been documented in a few studies (Veerakumar et al., 2014). Guo et al. (2016) indicated that mesoporous carbon coupled plasmonic gold nanoparticles coupled with $NaBH_4$ function as an outstanding catalyst for the transformation of p-nitrophenol to p-aminophenol. The hybridization with other plasmonic organisms, non-metals and metals of graphene and carbon nanotubes improves the nanomaterials' reactivity and reusability. Studies investigating the applicability of carbon functional materials have been published previously. Further various carbon-based materials are tabulated in Table 2.

Functional materials based upon zirconium

In the field of high-surface porous materials, zirconium-derived materials have expressed demanding promise in the rapid growth of material engineering. The zirconium (Tetragonal), architecture consisting of zirconium and benzenedicarboxylate, has been employed to engineering a metal-organic framework UiO-66. Due to its π-π interactions and ionic interactions, the substance has shown similar characteristics to carbon. Besides, these MOFs have excellent detection capabilities for organophosphates. The UiO-66 and 67 Zr-OH groups display a preference for pesticides such as glyphosate phosphates (Bugaev et al., 2018). Subsequently, the materials based on zirconium were used to enhance the photocatalyst's mesoporous property. Goswami and Ganguli (2013) stated the mitigation of quinalphos by zirconia/titania composite. The effect of zirconia doping allows oxygen vacancies to trap electrons and zirconia to trap holes, making them excellent electron separators. High activity zirconium content has also been reported to be involved in hydrogen production and photocatalysis by doping platinum (An et al., 2018).

Polymeric derived functional materials

In the field of water treatment, functional polymeric materials have gained a lot of interest. These materials can be synthetic or natural and can be modified to other components (Wang et al., 2013; Hu et al., 2015). In membrane preparation, many polymers are often used as immobilization substrates and resins to target particular pollutants in waste water (Halake et al., 2014). The extraction of materials such as chitosan, cellulose, alginate, and Cyclodextrins from plant, seashell residues such as shells, wood, leaves, etc. (Ding et al., 2009; Ngo et al., 2015). The functional biomaterials display more significant interaction of the adsorptive properties, functional group, and greater pollutant piling. Besides, these polymeric materials exhibit extraordinary stability and porosity and can be adjusted on the surface to improve their

interaction with pesticides. The formation of a layer from core shells allowing improved diffusion of pesticides, the simple design of biomaterials can be used for the layer. For the efficient removal of 2,4-Dinitrophenol, previous investigations have documented the adaptation of the NH_2 group of functionalized carbon coated with polyacrylonitrile. The adsorption of the anionic contaminants on the polymer cationic amino group is the intrinsic mechanism (Zhao et al., 2017). The adsorption of cationic contaminants as pesticides is strongly regulated by the molecule's pKa as negative charges that can interfere with the positive polymer are revealed by the greater dissociation of molecules above pKa. A versatile structure for contaminant removal and easy separation from the aqueous medium has also been documented for functional polymer materials such as β-cyclodextrin-chitosan-magnetic material, β-cyclodextrin-silica nanomaterial (Zhao et al., 2017). Metal-integrated polymers are successful in sorption execution as well as acting as a porous catalysis substrate. Advanced oxidation of organic contaminants occurs in functional polymers impregnated with gold and silver. Gold-polythiophene core-shell and silver citrate polymer materials are some of those materials (Pradeep, 2009). The model for casting flexible porous membranes that can be used as ultrafiltration and nano-filtration membranes can be made from biomaterials (Mukherjee et al., 2018). Besides, certain materials have been mimicking the sediment sorption mechanism of hydrophobic contaminants with natural clay minerals such as montmorillonite (MMT) (Sahithya et al., 2015; Foo, 2016; Shabtai and Mishael, 2017). Specific conductive polymers including polyaniline, polypyrrole, and polythiophene have flexible properties that can be used in photocatalytic membranes, such as electrical conductivity and semiconductor-based properties (Sarkar and Das, 2017; Khan et al., 2018). However, the problem of biofilm formation that leads to surface passivation is faced by polymeric materials used in membranes. Because of its antibacterial property, materials such as silver loaded

polymers may prohibit biofilm development. Biomaterials provide a low-cost alternative for developing flexible pesticide removal filters and membranes. In order to formulate unique biopolymers for targeting overdosed pesticides, the properties of membranes need to be examined in detail. The studies that developed carbon, zirconium and polymer based functional materials to treat pesticides consisting of are presented in Table 2.

Application of functional nanomaterials in industry

The application of polysaccharides and polymers can well be found via integrated membranes in oil separation mechanisms. In the manufacture of membranes, hydroxyethylcellulose, xanthan gums, guar gum, scleroglucan, cellulose, carboxymethylcellulose, etc. were used (Subash et al., 2013). For the elimination of inorganic and organic compounds from industrial waste water, the membranes may be used selectively. Industrial wastewater treatment requires that usable materials be tolerant of hazardous conditions. Fouling due to its antimicrobial nature is avoided using functional materials such as silver embedded carbon or polymers. The effect of high interfering ion concentrations induces shock loads to the effluent treatment easily controlled by practical material models for high surface area. Moreover, the spectrum of photocatalytic hybrids overcomes the conventional limitations that can be built to use solar light that degrade organics and hydrocarbons that are permanent. Besides, the regeneration of usable materials permits repeated reuse in industrial applications, lowering running costs (Grandclément et al., 2017). The use of materials in wastewater treatment as fine powders and pellets helps them absorb a wide variety of contaminants found in industrial wastewater, such as heavy metals, pesticides, antibiotics, surfactants, etc. (Kuśmierek and Świątkowski, 2015). In addition to the innovative production of usable materials from synthetic sources, industrial waste can also be developed to provide a sustainable alternative for sludge handling and reuse (Edathil et al., 2018).

Concluding remarks and future prospects

In conclusion, pesticide development and their effective utilization as per standard regulations have noteworthy contributions in fulfilling the ever-rising food demand. However, the disproportionate and inconsistent/irregular use of any or many pesticides that include bactericides, fungicides, herbicides, insecticides, and so on pose severe environmental and biological effects on plants, animals, and humans. Such massive consumption avoiding the standard regulations creates havoc on living beings and alters the whole ecological structure. In this context, the short and long-term consequences of pesticide compounds and/or their active by-products or residues that ultimately get discharged into water matrices should be considered with care before their agricultural or aquacultural exploitation. Moreover, the environmental and water matrices are at substantial threat of contamination due to pesticide drift, such as vapor drift and leaching drift after post-application into air or water bodies, respectively. After years of negligence, now the adverse consequences are evident in several diseases, such as cancer and other chronic diseases, and these are still emerging at a high pace. As discussed above in respective sections, many of these diseases are attributed to the consistent use and bioaccumulation of pesticide compounds in our system, which act as a catalyst to carcinogens and other disease-stimulating active agents.

There is a dire need to mitigate pesticide contamination for a safe and better tomorrow. Thus, keeping this in mind, this article spotlights the functional attributes of tailored functional materials as robust candidates since conventional methods have several limitations for removing the pesticides. The work is enriched with several functional materials with suitable examples and their exploitation against different pesticidal compounds. Based on the above-discussed literature with relevant examples, it is evident that integrating tailored functional materials as robust

candidates could be useful to mitigate pesticides from wastewater matrices. However, their large-scale implementation in bulk seems a formidable challenge, and intensive research investigations and cost-effective models are of supreme interest for future studies. Given that increasing the exploitation of tailored functional materials-based mitigation systems for pesticides drives at the cost of low reliability and efficacy and that such mitigation systems are still in their infancy and urge substantial advancement in the coming future.

Acknowledgments

Consejo Nacional de Ciencia y Tecnología (MX) is thankfully acknowledged for partially supporting this work under Sistema Nacional de Investigadores (SNI) program awarded to Hafiz M.N. Iqbal (CVU: 735340). The representative universities or institutes are thankfully acknowledged for providing literature services.

Conflict of interest disclosure

The representative authors have no conflict of interest to disclose in any capacity, either competing or financial.

References

Abbas, T., Wadhawan, T., Khan, A., McEvoy, J., Khan, E., 2020. Virgin (Fe0) and microbially regenerated (Fe^{2+}) iron turning waste for treating chlorinated pesticides in water. Journal of Hazardous Materials 398, 122980.

Abukhadra, M.R., El-Sherbeeny, A.M., El-Meligy, M.A., Luqman, M., 2021. Insight into carbohydrate polymers (chitosan and 2-hydroxyethyl methacrylate/methyl methacrylate) intercalated bentonite-based nanocomposites as multifunctional and environmental adsorbents for methyl parathion pesticide. International Journal of Biological Macromolecules 167, 335-344.

529 Adabavazeh, H., Saljooqi, A., Shamspur, T., Mostafavi, A., 2021. Synthesis of polyaniline
530 decorated with ZnO and $CoMoO_4$ nanoparticles for enhanced photocatalytic degradation of
531 imidacloprid pesticide under visible light. Polyhedron 198, 115058.
532 Adachi, M., Murata, Y., Takao, J., Jiu, J., Sakamoto, M., Wang, F., 2004. Highly efficient dye-
533 sensitized solar cells with a titania thin-film electrode composed of a network structure of single-
534 crystal-like TiO_2 nanowires made by the "oriented attachment" mechanism. Journal of the
535 American Chemical Society 126, 14943-14949.
536 Agarwal, S., Sadeghi, N., Tyagi, I., Gupta, V.K., Fakhri, A., 2016. Adsorption of toxic
537 carbamate pesticide oxamyl from liquid phase by newly synthesized and characterized graphene
538 quantum dots nanomaterials. Journal of colloid and interface science 478, 430-438.
539 Aktar, M.W., Sengupta, D., Chowdhury, A., 2009. Impact of pesticides use in agriculture: their
540 benefits and hazards. Interdisciplinary toxicology 2, 1-12.
541 Al-Hamdi, A.M., Sillanpää, M., Bora, T., Dutta, J., 2016. Efficient photocatalytic degradation of
542 phenol in aqueous solution by SnO_2: Sb nanoparticles. Applied Surface Science 370, 229-236.
543 Al Hattab, M.T., Ghaly, A.E., 2012. Disposal and treatment methods for pesticide containing
544 wastewaters: critical review and comparative analysis. Journal of environmental protection 3,
545 431-453.
546 Alalm, M.G., Ookawara, S., Fukushi, D., Sato, A., Tawfik, A., 2016. Improved WO3
547 photocatalytic efficiency using ZrO_2 and Ru for the degradation of carbofuran and ampicillin.
548 Journal of hazardous materials 302, 225-231.
549 Alam, U., Khan, A., Raza, W., Khan, A., Bahnemann, D., Muneer, M., 2017. Highly efficient Y
550 and V co-doped ZnO photocatalyst with enhanced dye sensitized visible light photocatalytic
551 activity. Catalysis Today 284, 169-178.

552 Albay, C., Koç, M., Altın, İ., Bayrak, R., Değirmencioğlu, İ., Sökmen, M., 2016. New dye
553 sensitized photocatalysts: Copper (II)-phthalocyanine/TiO_2 nanocomposite for water
554 remediation. Journal of Photochemistry and Photobiology A: Chemistry 324, 117-125.
555 Ali, I., Alothman, Z., Al-Warthan, A., 2016. Sorption, kinetics and thermodynamics studies of
556 atrazine herbicide removal from water using iron nano-composite material. International journal
557 of environmental science and technology 13, 733-742.
558 An, M., Li, L., Tian, Y., Yu, H., Zhou, Q., 2018. The three-dimensional ordered macroporous
559 structure of the Pt/TiO 2–ZrO_2 composite enhanced its photocatalytic performance for the
560 photodegradation and photolysis of water. RSC advances 8, 18870-18879.
561 Anandan, S., Vinu, A., Lovely, K.S., Gokulakrishnan, N., Srinivasu, P., Mori, T., Murugesan,
562 V., Sivamurugan, V., Ariga, K., 2007a. Photocatalytic activity of La-doped ZnO for the
563 degradation of monocrotophos in aqueous suspension. Journal of Molecular Catalysis A:
564 Chemical 266, 149-157.
565 Anandan, S., Vinu, A., Mori, T., Gokulakrishnan, N., Srinivasu, P., Murugesan, V., Ariga, K.,
566 2007b. Photocatalytic degradation of 2, 4, 6-trichlorophenol using lanthanum doped ZnO in
567 aqueous suspension. Catalysis Communications 8, 1377-1382.
568 Aslam, M., Ismail, I.M., Chandrasekaran, S., Hameed, A., 2014. Morphology controlled bulk
569 synthesis of disc-shaped WO3 powder and evaluation of its photocatalytic activity for the
570 degradation of phenols. Journal of hazardous materials 276, 120-128.
571 Aslam, M., Soomro, M.T., Ismail, I.M., Salah, N., Gondal, M., Hameed, A., 2015. Sunlight
572 mediated removal of chlorophenols over tungsten supported ZnO: electrochemical and
573 photocatalytic studies. Journal of Environmental Chemical Engineering 3, 1901-1911.

574 Ayad, M.M., Amer, W.A., Kotp, M.G., 2017. Magnetic polyaniline-chitosan nanocomposite
575 decorated with palladium nanoparticles for enhanced catalytic reduction of 4-nitrophenol.
576 Molecular Catalysis 439, 72-80.
577 Banić, N., Abramović, B., Krstić, J., Šojić, D., Lončarević, D., Cherkezova-Zheleva, Z.,
578 Guzsvány, V., 2011. Photodegradation of thiacloprid using Fe/TiO_2 as a heterogeneous photo-
579 Fenton catalyst. Applied Catalysis B: Environmental 107, 363-371.
580 Banić, N.D., Abramović, B.F., Krstić, J.B., Šojić Merkulov, D.V., Finčur, N.L., Mitrić, M.N.,
581 2019. Novel WO_3/Fe_3O_4 magnetic photocatalysts: Preparation, characterization and thiacloprid
582 photodegradation. Journal of Industrial and Engineering Chemistry 70, 264-275.
583 Bayantong, A.R.B., Shih, Y.-J., Ong, D.C., Abarca, R.R.M., Dong, C.-D., de Luna, M.D.G.,
584 2021. Adsorptive removal of dye in wastewater by metal ferrite-enabled graphene oxide
585 nanocomposites. Chemosphere 274, 129518.
586 Bechambi, O., Chalbi, M., Najjar, W., Sayadi, S., 2015. Photocatalytic activity of ZnO doped
587 with Ag on the degradation of endocrine disrupting under UV irradiation and the investigation of
588 its antibacterial activity. Applied Surface Science 347, 414-420.
589 Belessi, V., Lambropoulou, D., Konstantinou, I., Zboril, R., Tucek, J., Jancik, D., Albanis, T.,
590 Petridis, D., 2009. Structure and photocatalytic performance of magnetically separable titania
591 photocatalysts for the degradation of propachlor. Applied Catalysis B: Environmental 87, 181-
592 189.
593 Boruah, P. K., Darabdhara, G., Das, M. R., 2021. Polydopamine functionalized graphene sheets
594 decorated with magnetic metal oxide nanoparticles as efficient nanozyme for the detection and
595 degradation of harmful triazine pesticides. Chemosphere 268, 129328.

596 Boruah, P.K., Sharma, B., Hussain, N., Das, M.R., 2017. Magnetically recoverable
597 Fe_3O_4/graphene nanocomposite towards efficient removal of triazine pesticides from aqueous
598 solution: investigation of the adsorption phenomenon and specific ion effect. Chemosphere 168,
599 1058-1067.
600 Boucher, J., Steiner, L., Marison, I., 2007. Bio-sorption of atrazine in the press-cake from
601 oilseeds. Water research 41, 3209-3216.
602 Bugaev, A., Guda, A.A., Lomachenko, K.A., Kamyshova, E.G., Soldatov, M.A., Kaur, G., Øien-
603 Ødegaard, S., Braglia, L., Lazzarini, A., Manzoli, M., 2018. Operando study of palladium
604 nanoparticles inside UiO-67 MOF for catalytic hydrogenation of hydrocarbons. Faraday
605 Discussions 208, 287-306.
606 Cai, Y.-q., Cai, Y.-e., Mou, S.-f., Lu, Y.-q., 2005. Multi-walled carbon nanotubes as a solid-
607 phase extraction adsorbent for the determination of chlorophenols in environmental water
608 samples. Journal of Chromatography A 1081, 245-247.
609 Cao, J., Elliott, D., Zhang, W.-x., 2005. Perchlorate reduction by nanoscale iron particles.
610 Journal of Nanoparticle Research 7, 499-506.
611 Cao, Y., Tan, H., Shi, T., Tang, T., Li, J., 2008. Preparation of Ag-doped TiO_2 nanoparticles for
612 photocatalytic degradation of acetamiprid in water. Journal of Chemical Technology &
613 Biotechnology: International Research in Process, Environmental & Clean Technology 83, 546-
614 552.
615 Chen, G.-C., Shan, X.-Q., Zhou, Y.-Q., Shen, X.-e., Huang, H.-L., Khan, S.U., 2009. Adsorption
616 kinetics, isotherms and thermodynamics of atrazine on surface oxidized multiwalled carbon
617 nanotubes. Journal of Hazardous Materials 169, 912-918.

618 Chen, H., Yang, S., Yu, K., Ju, Y., Sun, C., 2011. Effective photocatalytic degradation of
619 atrazine over titania-coated carbon nanotubes (CNTs) coupled with microwave energy. The
620 Journal of Physical Chemistry A 115, 3034-3041.
621 Chiou, J.-R., Lai, B.-H., Hsu, K.-C., Chen, D.-H., 2013. One-pot green synthesis of silver/iron
622 oxide composite nanoparticles for 4-nitrophenol reduction. Journal of hazardous materials 248,
623 394-400.
624 Chitose, N., Ueta, S., Seino, S., Yamamoto, T.A., 2003. Radiolysis of aqueous phenol solutions
625 with nanoparticles. 1. Phenol degradation and TOC removal in solutions containing TiO2
626 induced by UV, γ-ray and electron beams. Chemosphere 50, 1007-1013.
627 Cho, S., Ahn, C., Park, J., Jeon, S., 2018. 3D nanostructured N-doped TiO_2 photocatalysts with
628 enhanced visible absorption. Nanoscale 10, 9747-9751.
629 Comparelli, R., Fanizza, E., Curri, M., Cozzoli, P., Mascolo, G., Agostiano, A., 2005. UV-
630 induced photocatalytic degradation of azo dyes by organic-capped ZnO nanocrystals
631 immobilized onto substrates. Applied Catalysis B: Environmental 60, 1-11.
632 Cui, X., Tian, L., Xian, X., Tang, H., Yang, X., 2018. Solar photocatalytic water oxidation over
633 Ag_3PO_4/g-C_3N_4 composite materials mediated by metallic Ag and graphene. Applied Surface
634 Science 430, 108-115.
635 Darwish, M., Mohammadi, A., Assi, N., Manuchehri, Q.S., Alahmad, Y., Abuzerr, S., 2017.
636 Shape-controlled ZnO nanocrystals synthesized via auto combustion method and enhancement of
637 the visible light catalytic activity by decoration on graphene. Journal of Alloys and Compounds
638 703, 396-406.
639 Debnath, D., Gupta, A.K., 2018. Optimizing the fabrication of nano-plasmonic silver-nitrogen
640 co-doped zinc oxide (AgxZn (1-x) NyO (1-y)) mediated by ammonia template: Insight into its

641 enhanced physiochemical and photocatalytic behavior. Journal of Molecular Liquids 249, 334-
642 345.
643 Debnath, D., Gupta, A.K., Ghosal, P.S., 2019. Recent advances in the development of tailored
644 functional materials for the treatment of pesticides in aqueous media: A review. Journal of
645 Industrial and Engineering Chemistry 70, 51-69.
646 Dehaghi, S.M., Rahmanifar, B., Moradi, A.M., Azar, P.A., 2014. Removal of permethrin
647 pesticide from water by chitosan–zinc oxide nanoparticles composite as an adsorbent. Journal of
648 Saudi Chemical Society 18, 348-355.
649 Ding, Y., Zhao, Y., Tao, X., Zheng, Y.-Z., Chen, J.-F., 2009. Assembled alginate/chitosan
650 micro-shells for removal of organic pollutants. Polymer 50, 2841-2846.
651 Ding, Y., Zhu, L., Wang, N., Tang, H., 2013. Sulfate radicals induced degradation of
652 tetrabromobisphenol A with nanoscaled magnetic $CuFe_2O_4$ as a heterogeneous catalyst of
653 peroxymonosulfate. Applied Catalysis B: Environmental 129, 153-162.
654 Divband, B., Khatamian, M., Eslamian, G.K., Darbandi, M., 2013. Synthesis of Ag/ZnO
655 nanostructures by different methods and investigation of their photocatalytic efficiency for 4-
656 nitrophenol degradation. Applied surface science 284, 80-86.
657 Dong, R., Tian, B., Zeng, C., Li, T., Wang, T., Zhang, J., 2013. Ecofriendly synthesis and
658 photocatalytic activity of uniform cubic Ag@ AgCl plasmonic photocatalyst. The Journal of
659 Physical Chemistry C 117, 213-220.
660 Edathil, A.A., Pal, P., Banat, F., 2018. Alginate clay hybrid composite adsorbents for the
661 reclamation of industrial lean methyldiethanolamine solutions. Applied Clay Science 156, 213-
662 223.

Elliott, D.W., Lien, H.-L., Zhang, W.-X., 2009. Degradation of lindane by zero-valent iron nanoparticles. Journal of Environmental Engineering 135, 317-324.

Fard, M.A., Vosoogh, A., Barkdoll, B., Aminzadeh, B., 2017. Using polymer coated nanoparticles for adsorption of micropollutants from water. Colloids and Surfaces A: Physicochemical and Engineering Aspects 531, 189-197.

Feng, J., Su, L., Ma, Y., Ren, C., Guo, Q., Chen, X., 2013. $CuFe_2O_4$ magnetic nanoparticles: A simple and efficient catalyst for the reduction of nitrophenol. Chemical engineering journal 221, 16-24.

Follut, F., Leitner, N.K.V., 2007. Radiolysis of aqueous 4-nitrophenol solution with Al_2O_3 or TiO_2 nanoparticles. Chemosphere 66, 2114-2119.

Foo, K., 2016. Value-added utilization of maize cobs waste as an environmental friendly solution for the innovative treatment of carbofuran. Process Safety and Environmental Protection 100, 295-304.

Gao, B., Liu, L., Liu, J., Yang, F., 2013. Photocatalytic degradation of 2, 4, 6-tribromophenol over Fe-doped $ZnIn_2S_4$: Stable activity and enhanced debromination. Applied Catalysis B: Environmental 129, 89-97.

Garcia-Muñoz, P., Fresno, F., Ivanez, J., Robert, D., Keller, N., 2020. Activity enhancement pathways in $LaFeO_3$@TiO_2 heterojunction photocatalysts for visible and solar light driven degradation of myclobutanil pesticide in water. Journal of Hazardous Materials 400, 123099.

Ghanbarlou, H., Nasernejad, B., Nikbakht Fini, M., Simonsen, M.E., Muff, J., 2020. Synthesis of an iron-graphene based particle electrode for pesticide removal in three-dimensional heterogeneous electro-Fenton water treatment system. Chemical Engineering Journal 395, 125025.

686 Goswami, P., Ganguli, J.N., 2013. Tuning the band gap of mesoporous Zr-doped TiO_2 for
687 effective degradation of pesticide quinalphos. Dalton Transactions 42, 14480-14490.
688 Grandclément, C., Seyssiecq, I., Piram, A., Wong-Wah-Chung, P., Vanot, G., Tiliacos, N.,
689 Roche, N., Doumenq, P., 2017. From the conventional biological wastewater treatment to hybrid
690 processes, the evaluation of organic micropollutant removal: a review. Water research 111, 297-
691 317.
692 Graymore, M., Stagnitti, F., Allinson, G., 2001. Impacts of atrazine in aquatic ecosystems.
693 Environment international 26, 483-495.
694 Grundlingh, J., Dargan, P.I., El-Zanfaly, M., Wood, D.M., 2011. 2, 4-dinitrophenol (DNP): a
695 weight loss agent with significant acute toxicity and risk of death. Journal of medical toxicology
696 7, 205.
697 Gulati, A., Mandeep, Malik, J., Kakkar, R., 2020. Mesoporous rGO@ZnO composite: Facile
698 synthesis and excellent water treatment performance by pesticide adsorption and catalytic
699 oxidative dye degradation. Chemical Engineering Research and Design 160, 254-263.
700 Guo, P., Tang, L., Tang, J., Zeng, G., Huang, B., Dong, H., Zhang, Y., Zhou, Y., Deng, Y., Ma,
701 L., 2016. Catalytic reduction–adsorption for removal of p-nitrophenol and its conversion p-
702 aminophenol from water by gold nanoparticles supported on oxidized mesoporous carbon.
703 Journal of colloid and interface science 469, 78-85.
704 Gupta, A., Pal, A., Sahoo, C., 2006. Photocatalytic degradation of a mixture of Crystal Violet
705 (Basic Violet 3) and Methyl Red dye in aqueous suspensions using Ag+ doped TiO_2. Dyes and
706 Pigments 69, 224-232.
707 Gupta, V., Gupta, B., Rastogi, A., Agarwal, S., Nayak, A., 2011. Pesticides removal from waste
708 water by activated carbon prepared from waste rubber tire. Water research 45, 4047-4055.

709 Gupta, V.K., Eren, T., Atar, N., Yola, M.L., Parlak, C., Karimi-Maleh, H., 2015. $CoFe_2O_4$@
710 TiO_2 decorated reduced graphene oxide nanocomposite for photocatalytic degradation of
711 chlorpyrifos. Journal of Molecular Liquids 208, 122-129.
712 Gutiérrez-Jara, J.P., Córdova-Lepe, F.D., Muñoz-Quezada, M.T., Chowell, G., 2020.
713 Susceptibility to organophosphates pesticides and the development of infectious-contagious
714 respiratory diseases. Journal of Theoretical Biology 488, 110133.
715 Halake, K., Birajdar, M., Kim, B.S., Bae, H., Lee, C., Kim, Y.J., Kim, S., Kim, H.J., Ahn, S.,
716 An, S.Y., 2014. Recent application developments of water-soluble synthetic polymers. Journal of
717 Industrial and Engineering Chemistry 20, 3913-3918.
718 Hashimoto, S., Matsukami, H., Ieda, T., Suzuki, G., 2021. Comprehensive screening of
719 polybromochlorodibenzo-p-dioxins, dibenzofurans as mixed halogenated compounds in
720 wastewater samples from industrial facilities by GC×GC/ToFMS and post-data processing.
721 Chemosphere, 130085.
722 He, F., Zhao, D., 2005. Preparation and characterization of a new class of starch-stabilized
723 bimetallic nanoparticles for degradation of chlorinated hydrocarbons in water. Environmental
724 science & technology 39, 3314-3320.
725 Hernández-Gordillo, A., González, V.R., 2015. Silver nanoparticles loaded on Cu-doped TiO_2
726 for the effective reduction of nitro-aromatic contaminants. Chemical Engineering Journal 261,
727 53-59.
728 Hossaini, H., Moussavi, G., Farrokhi, M., 2014. The investigation of the LED-activated FeFNS-
729 TiO_2 nanocatalyst for photocatalytic degradation and mineralization of organophosphate
730 pesticides in water. Water research 59, 130-144.

731 Hu, R., Dai, S., Shao, D., Alsaedi, A., Ahmad, B., Wang, X., 2015. Efficient removal of phenol
732 and aniline from aqueous solutions using graphene oxide/polypyrrole composites. Journal of
733 Molecular Liquids 203, 80-89.
734 Huang, D., Tang, Z., Peng, Z., Lai, C., Zeng, G., Zhang, C., Xu, P., Cheng, M., Wan, J., Wang,
735 R., 2017. Fabrication of water-compatible molecularly imprinted polymer based on β-
736 cyclodextrin modified magnetic chitosan and its application for selective removal of bisphenol A
737 from aqueous solution. Journal of the Taiwan Institute of Chemical Engineers 77, 113-121.
738 Huo, P., Liu, C., Wu, D., Guan, J., Li, J., Wang, H., Tang, Q., Li, X., Yan, Y., Yuan, S., 2018.
739 Fabricated Ag/Ag_2S/reduced graphene oxide composite photocatalysts for enhancing visible
740 light photocatalytic and antibacterial activity. Journal of industrial and engineering chemistry 57,
741 125-133.
742 Ibrahim, S., Chakrabarty, S., Ghosh, S., Pal, T., 2017. Reduced graphene oxide–zinc sulfide
743 composite for solar light responsive photo current generation and photocatalytic 4-nitrophenol
744 reduction. ChemistrySelect 2, 537-545.
745 Ishihara, A., Nishiyama, N., Sugiyama, S.-i., Yamauchi, K., 2003. The effect of endocrine
746 disrupting chemicals on thyroid hormone binding to Japanese quail transthyretin and thyroid
747 hormone receptor. General and comparative endocrinology 134, 36-43.
748 Ismail, A.A., Abdelfattah, I., Helal, A., Al-Sayari, S., Robben, L., Bahnemann, D., 2016. Ease
749 synthesis of mesoporous WO_3–TiO_2 nanocomposites with enhanced photocatalytic performance
750 for photodegradation of herbicide imazapyr under visible light and UV illumination. Journal of
751 hazardous materials 307, 43-54.

752 Jeon, E.K., Seo, E., Lee, E., Lee, W., Um, M.-K., Kim, B.-S., 2013. Mussel-inspired green
753 synthesis of silver nanoparticles on graphene oxide nanosheets for enhanced catalytic
754 applications. Chemical communications 49, 3392-3394.
755 Jiang, Z., Jiang, D., Hossain, A.S., Qian, K., Xie, J., 2015. In situ synthesis of silver supported
756 nanoporous iron oxide microbox hybrids from metal–organic frameworks and their catalytic
757 application in p-nitrophenol reduction. Physical Chemistry Chemical Physics 17, 2550-2559.
758 Jonidi-Jafari, A., Shirzad-Siboni, M., Yang, J.-K., Naimi-Joubani, M., Farrokhi, M., 2015.
759 Photocatalytic degradation of diazinon with illuminated ZnO–TiO_2 composite. Journal of the
760 Taiwan institute of chemical engineers 50, 100-107.
761 Joo, S.H., Zhao, D., 2008. Destruction of lindane and atrazine using stabilized iron nanoparticles
762 under aerobic and anaerobic conditions: effects of catalyst and stabilizer. Chemosphere 70, 418-
763 425.
764 Justh, N., Firkala, T., László, K., Lábár, J., Szilágyi, I.M., 2017. Photocatalytic C60-amorphous
765 TiO_2 composites prepared by atomic layer deposition. Applied Surface Science 419, 497-502.
766 Karabelas, A., Plakas, K., Solomou, E., Drossou, V., Sarigiannis, D., 2009. Impact of European
767 legislation on marketed pesticides—a view from the standpoint of health impact assessment
768 studies. Environment international 35, 1096-1107.
769 Keshvardoostchokami, M., Bigverdi, P., Zamani, A., Parizanganeh, A., Piri, F., 2018. Silver@
770 graphene oxide nanocomposite: synthesize and application in removal of imidacloprid from
771 contaminated waters. Environmental Science and Pollution Research 25, 6751-6761.
772 Keum, Y.-S., Li, Q.X., 2004. Reduction of nitroaromatic pesticides with zero-valent iron.
773 Chemosphere 54, 255-263.

774 Khajeh, M., Laurent, S., Dastafkan, K., 2013. Nanoadsorbents: classification, preparation, and
775 applications (with emphasis on aqueous media). Chemical reviews 113, 7728-7768.
776 Khan, A., Khan, A.A.P., Rahman, M.M., Asiri, A.M., Alamry, K.A., Hameed, S.A., 2018.
777 Preparation and characterization of PANI@ G/CWO nanocomposite for enhanced 2-nitrophenol
778 sensing. Applied Surface Science 433, 696-704.
779 Khatamian, M., Khandar, A., Divband, B., Haghighi, M., Ebrahimiasl, S., 2012. Heterogeneous
780 photocatalytic degradation of 4-nitrophenol in aqueous suspension by Ln (La^{3+}, Nd^{3+} or Sm^{3+})
781 doped ZnO nanoparticles. Journal of Molecular Catalysis A: Chemical 365, 120-127.
782 Kodali, J., Talasila, S., Arunraj, B., Nagarathnam, R., 2021. Activated Coconut Charcoal as a
783 Super Adsorbent for the Removal of Organophosphorous Pesticide Monocrotophos from Water.
784 Case Studies in Chemical and Environmental Engineering, 100099.
785 Konstantinou, I.K., Hela, D.G., Albanis, T.A., 2006. The status of pesticide pollution in surface
786 waters (rivers and lakes) of Greece. Part I. Review on occurrence and levels. Environmental
787 Pollution 141, 555-570.
788 Korake, P., Dhabbe, R., Kadam, A., Gaikwad, Y., Garadkar, K., 2014. Highly active lanthanum
789 doped ZnO nanorods for photodegradation of metasystox. Journal of Photochemistry and
790 Photobiology B: Biology 130, 11-19.
791 Korake, P., Sridharkrishna, R., Hankare, P., Garadkar, K., 2012. Photocatalytic degradation of
792 phosphamidon using Ag-doped ZnO nanorods. Toxicological & Environmental Chemistry 94,
793 1075-1085.
794 Kumar, A., Naushad, M., Rana, A., Sharma, G., Ghfar, A.A., Stadler, F.J., Khan, M.R., 2017.
795 ZnSe-WO_3 nano-hetero-assembly stacked on Gum ghatti for photo-degradative removal of

Bisphenol A: Symbiose of adsorption and photocatalysis. International journal of biological macromolecules 104, 1172-1184.

Kumar, S.G., Rao, K.K., 2015. Zinc oxide based photocatalysis: tailoring surface-bulk structure and related interfacial charge carrier dynamics for better environmental applications. Rsc Advances 5, 3306-3351.

Kurian, M., Kunjachan, C., Sreevalsan, A., 2017. Catalytic degradation of chlorinated organic pollutants over CexFe1− xO2 (x: 0, 0.25, 0.5, 0.75, 1) nanocomposites at mild conditions. Chemical Engineering Journal 308, 67-77.

Kuśmierek, K., Świątkowski, A., 2015. The influence of different agitation techniques on the adsorption kinetics of 4-chlorophenol on granular activated carbon. Reaction Kinetics, Mechanisms and Catalysis 116, 261-271.

Lam, S.-M., Sin, J.-C., Satoshi, I., Abdullah, A.Z., Mohamed, A.R., 2014. Enhanced sunlight photocatalytic performance over Nb_2O_5/ZnO nanorod composites and the mechanism study. Applied Catalysis A: General 471, 126-135.

Lee, H.-G., Sai-Anand, G., Komathi, S., Gopalan, A.-I., Kang, S.-W., Lee, K.-P., 2015. Efficient visible-light-driven photocatalytic degradation of nitrophenol by using graphene-encapsulated TiO_2 nanowires. Journal of hazardous materials 283, 400-409.

Lee, J.S., Jang, J., 2014. Hetero-structured semiconductor nanomaterials for photocatalytic applications. Journal of Industrial and Engineering Chemistry 20, 363-371.

Lee, S.-Y., Park, S.-J., 2013. TiO_2 photocatalyst for water treatment applications. Journal of Industrial and Engineering Chemistry 19, 1761-1769.

817 Lee, S.C., Lintang, H.O., Yuliati, L., 2017. High photocatalytic activity of Fe2O3/TiO2
818 nanocomposites prepared by photodeposition for degradation of 2, 4-dichlorophenoxyacetic acid.
819 Beilstein journal of nanotechnology 8, 915-926.
820 Lee, Y.-J., Chang, Y.-J., Lee, D.-J., Hsu, J.-P., 2018. Water stable metal-organic framework as
821 adsorbent from aqueous solution: A mini-review. Journal of the Taiwan Institute of Chemical
822 Engineers 93, 176-183.
823 Lin, Y.-S., Wu, S.-H., Hung, Y., Chou, Y.-H., Chang, C., Lin, M.-L., Tsai, C.-P., Mou, C.-Y.,
824 2006. Multifunctional composite nanoparticles: magnetic, luminescent, and mesoporous.
825 Chemistry of Materials 18, 5170-5172.
826 Linsebigler, A.L., Lu, G., Yates Jr, J.T., 1995. Photocatalysis on TiO_2 surfaces: principles,
827 mechanisms, and selected results. Chemical reviews 95, 735-758.
828 Liu, G., Li, L., Xu, D., Huang, X., Xu, X., Zheng, S., Zhang, Y., Lin, H., 2017. Metal–organic
829 framework preparation using magnetic graphene oxide–β-cyclodextrin for neonicotinoid
830 pesticide adsorption and removal. Carbohydrate polymers 175, 584-591.
831 Liu, L., Chen, F., Yang, F., Chen, Y., Crittenden, J., 2012. Photocatalytic degradation of 2, 4-
832 dichlorophenol using nanoscale Fe/TiO_2. Chemical Engineering Journal 181, 189-195.
833 López-Ayala, S., Rincón, M., Alfaro, M.Q., Bandala, E., Rojas, M.M., Castano, V., 2015.
834 Nanocrystalline titania xerogels doped by metal precursors in the photocatalytic degradation of
835 2, 4-D sodium salts. Journal of Photochemistry and Photobiology A: Chemistry 311, 166-175.
836 Luo, B., Xu, D., Li, D., Wu, G., Wu, M., Shi, W., Chen, M., 2015. Fabrication of a Ag/Bi3TaO7
837 plasmonic photocatalyst with enhanced photocatalytic activity for degradation of tetracycline.
838 ACS applied materials & interfaces 7, 17061-17069.

Maleki, A., Moradi, F., Shahmoradi, B., Rezaee, R., Lee, S.-M., 2020. The photocatalytic removal of diazinon from aqueous solutions using tungsten oxide doped zinc oxide nanoparticles immobilized on glass substrate. Journal of Molecular Liquids 297, 111918.

Maya-Treviño, M., Guzmán-Mar, J., Hinojosa-Reyes, L., Ramos-Delgado, N., Maldonado, M., Hernández-Ramírez, A., 2014. Activity of the ZnO–Fe_2O_3 catalyst on the degradation of Dicamba and 2, 4-D herbicides using simulated solar light. Ceramics International 40, 8701-8708.

Mbiri, A., Wittstock, G., Taffa, D.H., Gatebe, E., Baya, J., Wark, M., 2018. Photocatalytic degradation of the herbicide chloridazon on mesoporous titania/zirconia nanopowders. Environmental Science and Pollution Research 25, 34873-34883.

McKinlay, R., Plant, J., Bell, J., Voulvoulis, N., 2008. Endocrine disrupting pesticides: implications for risk assessment. Environment international 34, 168-183.

Meshram, S., Limaye, R., Ghodke, S., Nigam, S., Sonawane, S., Chikate, R., 2011. Continuous flow photocatalytic reactor using ZnO–bentonite nanocomposite for degradation of phenol. Chemical Engineering Journal 172, 1008-1015.

Mirmasoomi, S.R., Ghazi, M.M., Galedari, M., 2017. Photocatalytic degradation of diazinon under visible light using TiO_2/Fe_2O_3 nanocomposite synthesized by ultrasonic-assisted impregnation method. Separation and Purification Technology 175, 418-427.

Mkhalid, I., 2016. Photocatalytic degradation of herbicides under visible light using Pd-WO_3 nanorods. Ceramics International 42, 15975-15980.

Mohammad, S.G., El-Sayed, M.M., 2020. Removal of imidacloprid pesticide using nanoporous activated carbons produced via pyrolysis of peach stone agricultural wastes. Chemical Engineering Communications, 1-12.

862 Mohmood, I., Lopes, C.B., Lopes, I., Ahmad, I., Duarte, A.C., Pereira, E., 2013. Nanoscale
863 materials and their use in water contaminants removal—a review. Environmental science and
864 pollution Research 20, 1239-1260.
865 Mourabit, F., Boulaid, M., 2019. Pesticide removal in drinking water treatment using
866 biodegradable polymers. Materials Today: Proceedings 13, 1033-1038.
867 Moustafa, M., Abu-Saied, M., Taha, T., Elnouby, M., El-Shafeey, M., Alshehri, A.G., Alamri,
868 S., Shati, A., Alrumman, S., Alghamdii, H., 2021. Chitosan functionalized AgNPs for efficient
869 removal of Imidacloprid pesticide through a pressure-free design. International Journal of
870 Biological Macromolecules 168, 116-123.
871 Mukherjee, D., Bhattacharya, P., Jana, A., Bhattacharya, S., Sarkar, S., Ghosh, S., Majumdar, S.,
872 Swarnakar, S., 2018. Synthesis of ceramic ultrafiltration membrane and application in membrane
873 bioreactor process for pesticide remediation from wastewater. Process Safety and Environmental
874 Protection 116, 22-33.
875 Nagpal, V., Bokare, A.D., Chikate, R.C., Rode, C.V., Paknikar, K.M., 2010. Reductive
876 dechlorination of γ-hexachlorocyclohexane using Fe–Pd bimetallic nanoparticles. Journal of
877 hazardous materials 175, 680-687.
878 Naraginti, S., Stephen, F.B., Radhakrishnan, A., Sivakumar, A., 2015. Zirconium and silver co-
879 doped TiO_2 nanoparticles as visible light catalyst for reduction of 4-nitrophenol, degradation of
880 methyl orange and methylene blue. Spectrochimica Acta Part A: Molecular and Biomolecular
881 Spectroscopy 135, 814-819.
882 Narayanan, N., Gupta, S., Gajbhiye, V., 2020. Decontamination of pesticide industrial effluent
883 by adsorption–coagulation–flocculation process using biopolymer-nanoorganoclay composite.
884 International Journal of Environmental Science and Technology 17, 4775-4786.

885 Navarro, S., Fenoll, J., Vela, N., Ruiz, E., Navarro, G., 2009. Photocatalytic degradation of eight
886 pesticides in leaching water by use of ZnO under natural sunlight. Journal of hazardous materials
887 172, 1303-1310.
888 Nethaji, S., Sivasamy, A., 2017. Graphene oxide coated with porous iron oxide ribbons for 2, 4-
889 Dichlorophenoxyacetic acid (2, 4-D) removal. Ecotoxicology and environmental safety 138,
890 292-297.
891 Ngo, H.H., Guo, W., Zhang, J., Liang, S., Ton-That, C., Zhang, X., 2015. Typical low cost
892 biosorbents for adsorptive removal of specific organic pollutants from water. Bioresource
893 technology 182, 353-363.
894 Ogut, S., Kucukoner, E., Gultekin, F., Gurbuz, N., 2015. A study of long-term pesticide
895 application amongst agricultural workers: total antioxidant status, total oxidant status and
896 acetylcholinesterase activity in blood. Proceedings of the National Academy of Sciences, India
897 Section B: Biological Sciences 85, 155-159.
898 Pan, B., Xing, B., 2008. Adsorption mechanisms of organic chemicals on carbon nanotubes.
899 Environmental science & technology 42, 9005-9013.
900 Pan, J., Yao, H., Guan, W., Ou, H., Huo, P., Wang, X., Zou, X., Li, C., 2011. Selective
901 adsorption of 2, 6-dichlorophenol by surface imprinted polymers using polyaniline/silica gel
902 composites as functional support: equilibrium, kinetics, thermodynamics modeling. Chemical
903 engineering journal 172, 847-855.
904 Pankajakshan, A., Sinha, M., Ojha, A.A., Mandal, S., 2018. Water-stable nanoscale zirconium-
905 based metal–organic frameworks for the effective removal of glyphosate from aqueous media.
906 ACS omega 3, 7832-7839.

907 Panthi, G., Park, M., Kim, H.-Y., Lee, S.-Y., Park, S.-J., 2015. Electrospun ZnO hybrid
908 nanofibers for photodegradation of wastewater containing organic dyes: A review. Journal of
909 Industrial and Engineering Chemistry 21, 26-35.
910 Park, S.-H., Bae, J., 2015. Tailoring environment friendly carbon nanostructures by surfactant
911 mediated interfacial engineering. Journal of Industrial and Engineering Chemistry 30, 1-9.
912 Pei, Z., Ding, L., Lu, M., Fan, Z., Weng, S., Hu, J., Liu, P., 2014. Synergistic effect in
913 polyaniline-hybrid defective ZnO with enhanced photocatalytic activity and stability. The
914 Journal of Physical Chemistry C 118, 9570-9577.
915 Peng, X., Li, Y., Luan, Z., Di, Z., Wang, H., Tian, B., Jia, Z., 2003. Adsorption of 1, 2-
916 dichlorobenzene from water to carbon nanotubes. Chemical physics letters 376, 154-158.
917 Pillai, I.M.S., Gupta, A.K., 2016. Anodic oxidation of coke oven wastewater: multiparameter
918 optimization for simultaneous removal of cyanide, COD and phenol. Journal of Environmental
919 Management 176, 45-53.
920 Pillai, I.M.S., Gupta, A.K., Tiwari, M.K., 2015. Multivariate optimization for electrochemical
921 oxidation of methyl orange: pathway identification and toxicity analysis. Journal of
922 Environmental Science and Health, Part A 50, 301-310.
923 Pinto, M.d.C.E., Gonçalves, R.G.L., dos Santos, R.M.M., Araújo, E.A., Perotti, G.F., dos Santos
924 Macedo, R., Bizeto, M.A., Constantino, V.R.L., Pinto, F.G., Tronto, J., 2016. Mesoporous
925 carbon derived from a biopolymer and a clay: Preparation, characterization and application for
926 an organochlorine pesticide adsorption. Microporous and Mesoporous Materials 225, 342-354.
927 Pirhashemi, M., Habibi-Yangjeh, A., 2017. Preparation of novel nanocomposites by deposition
928 of Ag_2WO_4 and AgI over ZnO particles: efficient plasmonic visible-light-driven photocatalysts
929 through a cascade mechanism. Ceramics International 43, 13447-13460.

930 Pradeep, T., 2009. Noble metal nanoparticles for water purification: a critical review. Thin solid
931 films 517, 6441-6478.
932 Qamar, M.T., Aslam, M., Ismail, I.M., Salah, N., Hameed, A., 2015. Synthesis, characterization,
933 and sunlight mediated photocatalytic activity of CuO coated ZnO for the removal of
934 nitrophenols. ACS Applied Materials & Interfaces 7, 8757-8769.
935 Qin, H., Guo, W., Huang, X., Gao, P., Xiao, H., 2020. Preparation of yttria-stabilized ZrO_2
936 nanofiltration membrane by reverse micelles-mediated sol-gel process and its application in
937 pesticide wastewater treatment. Journal of the European Ceramic Society 40, 145-154.
938 Qu, X., Alvarez, P.J., Li, Q., 2013. Applications of nanotechnology in water and wastewater
939 treatment. Water research 47, 3931-3946.
940 Ramos-Delgado, N., Gracia-Pinilla, M., Maya-Trevino, L., Hinojosa-Reyes, L., Guzman-Mar, J.,
941 Hernández-Ramírez, A., 2013. Solar photocatalytic activity of TiO2 modified with WO3 on the
942 degradation of an organophosphorus pesticide. Journal of hazardous materials 263, 36-44.
943 Rana, V.K., Kissner, R., Jauregui-Haza, U., Gaspard, S., Levalois-Grützmacher, J., 2017.
944 Enhanced chlordecone (Kepone) removal by FeO-nanoparticles loaded on activated carbon.
945 Journal of environmental chemical engineering 5, 1608-1617.
946 Rani, M., Shanker, U., Jassal, V., 2017. Recent strategies for removal and degradation of
947 persistent & toxic organochlorine pesticides using nanoparticles: a review. Journal of
948 environmental management 190, 208-222.
949 Ranjbar Bandforuzi, S., Hadjmohammadi, M.R., 2019. Modified magnetic chitosan
950 nanoparticles based on mixed hemimicelle of sodium dodecyl sulfate for enhanced removal and
951 trace determination of three organophosphorus pesticides from natural waters. Analytica
952 Chimica Acta 1078, 90-100.

Reddy, P.A.K., Reddy, P.V.L., Kwon, E., Kim, K.-H., Akter, T., Kalagara, S., 2016. Recent advances in photocatalytic treatment of pollutants in aqueous media. Environment international 91, 94-103.

Reddy, P.V.L., Kim, K.-H., 2015. A review of photochemical approaches for the treatment of a wide range of pesticides. Journal of hazardous materials 285, 325-335.

Roshdy, A.A., Mady, A.H., Khalil, M.M.H., Abo-El-Enein, S.A., Elfadly, A.M., Lee, Y.-I., Yehia, F.Z., 2021. Novel polyaniline/tungsten trioxide@metal–organic framework nanocomposites for enhancing photodegradation of 4-nitrophenol. Environmental Technology & Innovation 22, 101404.

Sahithya, K., Das, D., Das, N., 2015. Effective removal of dichlorvos from aqueous solution using biopolymer modified MMT–CuO composites: equilibrium, kinetic and thermodynamic studies. Journal of Molecular Liquids 211, 821-830.

Sahoo, C., Gupta, A., 2012. Optimization of photocatalytic degradation of methyl blue using silver ion doped titanium dioxide by combination of experimental design and response surface approach. Journal of Hazardous Materials 215, 302-310.

Sahoo, C., Gupta, A.K., 2013. Application of statistical experimental design to optimize the photocatalytic degradation of a thiazin dye using silver ion-doped titanium dioxide. Journal of Environmental Science and Health, Part A 48, 694-705.

Sahoo, C., Gupta, A.K., 2015. Characterization and photocatalytic performance evaluation of various metal ion-doped microstructured TiO_2 under UV and visible light. Journal of Environmental Science and Health, Part A 50, 659-668.

Sarkar, S., Das, R., 2017. PVP capped silver nanocubes assisted removal of glyphosate from water—a photoluminescence study. Journal of hazardous materials 339, 54-62.

976 Senthilnathan, J., Philip, L., 2010. Removal of mixed pesticides from drinking water system
977 using surfactant-assisted nano-TiO_2. Water, Air, & Soil Pollution 210, 143-154.
978 Seo, Y.S., Khan, N.A., Jhung, S.H., 2015. Adsorptive removal of methylchlorophenoxypropionic
979 acid from water with a metal-organic framework. Chemical Engineering Journal 270, 22-27.
980 Shabtai, I.A., Mishael, Y.G., 2017. Catalytic polymer-clay composite for enhanced removal and
981 degradation of diazinon. Journal of hazardous materials 335, 135-142.
982 Shanmugam, V., Jeyaperumal, K.S., 2018. Investigations of visible light driven Sn and Cu doped
983 ZnO hybrid nanoparticles for photocatalytic performance and antibacterial activity. Applied
984 Surface Science 449, 617-630.
985 Sharma, A., Lee, B.-K., 2016. Rapid photo-degradation of 2-chlorophenol under visible light
986 irradiation using cobalt oxide-loaded TiO_2/reduced graphene oxide nanocomposite from aqueous
987 media. Journal of environmental management 165, 1-10.
988 Shi, H., Chen, J., Li, G., Nie, X., Zhao, H., Wong, P.-K., An, T., 2013. Synthesis and
989 characterization of novel plasmonic Ag/AgX-CNTs (X= Cl, Br, I) nanocomposite photocatalysts
990 and synergetic degradation of organic pollutant under visible light. ACS Applied Materials &
991 Interfaces 5, 6959-6967.
992 Shifu, C., Gengyu, C., 2005. Photocatalytic degradation of organophosphorus pesticides using
993 floating photocatalyst $TiO_2 \cdot SiO_2$/beads by sunlight. Solar Energy 79, 1-9.
994 Sin, J.-C., Lam, S.-M., Lee, K.-T., Mohamed, A.R., 2013. Preparation and photocatalytic
995 properties of visible light-driven samarium-doped ZnO nanorods. Ceramics International 39,
996 5833-5843.

997 Singh, S., Kaushal, S., Kaur, J., Kaur, G., Mittal, S.K., Singh, P.P., 2021. CaFu MOF as an
998 efficient adsorbent for simultaneous removal of imidacloprid pesticide and cadmium ions from
999 wastewater. Chemosphere 272, 129648.
1000 Sivagami, K., Vikraman, B., Krishna, R.R., Swaminathan, T., 2016. Chlorpyrifos and
1001 Endosulfan degradation studies in an annular slurry photo reactor. Ecotoxicology and
1002 environmental safety 134, 327-331.
1003 Slotkin, T., 1999. Developmental cholinotoxicants: nicotine and chlorpyrifos Environ Health
1004 Perspect 107 (suppl 1): 71–80. Find this article online.
1005 Soltani-nezhad, F., Saljooqi, A., Mostafavi, A., Shamspur, T., 2020. Synthesis of Fe_3O_4/CdS–
1006 ZnS nanostructure and its application for photocatalytic degradation of chlorpyrifos pesticide and
1007 brilliant green dye from aqueous solutions. Ecotoxicology and Environmental Safety 189,
1008 109886.
1009 Song, S., Cheng, B., Wu, N., Meng, A., Cao, S., Yu, J., 2016. Structure effect of graphene on the
1010 photocatalytic performance of plasmonic Ag/Ag_2CO_3-rGO for photocatalytic elimination of
1011 pollutants. Applied Catalysis B: Environmental 181, 71-78.
1012 Subash, B., Krishnakumar, B., Swaminathan, M., Shanthi, M., 2013. Highly efficient, solar
1013 active, and reusable photocatalyst: Zr-loaded Ag–ZnO for reactive red 120 dye degradation with
1014 synergistic effect and dye-sensitized mechanism. Langmuir 29, 939-949.
1015 Tahir, M.B., Nabi, G., Rafique, M., Khalid, N., 2017. Nanostructured-based WO_3 photocatalysts:
1016 recent development, activity enhancement, perspectives and applications for wastewater
1017 treatment. International Journal of Environmental Science and Technology 14, 2519-2542.
1018 Tang, L., Ma, X.Y., Wang, Y., Zhang, S., Zheng, K., Wang, X.C., Lin, Y., 2020. Removal of
1019 trace organic pollutants (pharmaceuticals and pesticides) and reduction of biological effects from

secondary effluent by typical granular activated carbon. Science of The Total Environment 749, 141611.

Tayour, C., Ritz, B., Langholz, B., Mills, P.K., Wu, A., Wilson, J.P., Shahabi, K., Cockburn, M., 2019. A case-control study of breast cancer risk and ambient exposure to pesticides. Environ Epidemiol 3, e070-e070.

Tee, Y.-H., Bachas, L., Bhattacharyya, D., 2009. Degradation of trichloroethylene by iron-based bimetallic nanoparticles. The Journal of Physical Chemistry C 113, 9454-9464.

Tian, B., Dong, R., Zhang, J., Bao, S., Yang, F., Zhang, J., 2014. Sandwich-structured AgCl@ Ag@ TiO2 with excellent visible-light photocatalytic activity for organic pollutant degradation and E. coli K12 inactivation. Applied Catalysis B: Environmental 158, 76-84.

Tian, H., Chen, J., He, J., Liu, F., 2015. Pd-loaded magnetic mesoporous nanocomposites: A magnetically recoverable catalyst with effective enrichment and high activity for DDT and DDE removal under mild conditions. Journal of Colloid and Interface Science 457, 195-202.

Tomer, V., Sangha, J.K., Ramya, H., 2015. Pesticide: An appraisal on human health implications. Proceedings of the National Academy of Sciences, India Section B: Biological Sciences 85, 451-463.

Tong, D., Zhuang, J., Lee, J., Buchanan, J., Chen, X., 2019. Concurrent transport and removal of nitrate, phosphate and pesticides in low-cost metal- and carbon-based materials. Chemosphere 230, 84-91.

Umukoro, E.H., Peleyeju, M.G., Ngila, J.C., Arotiba, O.A., 2017. Towards wastewater treatment: Photo-assisted electrochemical degradation of 2-nitrophenol and orange II dye at a tungsten trioxide-exfoliated graphite composite electrode. Chemical Engineering Journal 317, 290-301.

Vali, S.I., Sirisha, U., Poiba, V.R., Vangalapati, M., King, P., 2021. Synthesis and characterization of Titanium doped activated carbon nanoparticles and its application for the removal of dicofol. Materials Today: Proceedings.

Vaya, D., Surolia, P.K., 2020. Semiconductor based photocatalytic degradation of pesticides: An overview. Environmental Technology & Innovation, 101128.

Veerakumar, P., Madhu, R., Chen, S.-M., Veeramani, V., Hung, C.-T., Tang, P.-H., Wang, C.-B., Liu, S.-B., 2014. Highly stable and active palladium nanoparticles supported on porous carbon for practical catalytic applications. Journal of Materials Chemistry A 2, 16015-16022.

Wade T. J., Pai, N., Eisenberg Joseph, N.S., Colford John, M., 2003. Do U.S. Environmental Protection Agency water quality guidelines for recreational waters prevent gastrointestinal illness? A systematic review and meta-analysis. Environmental Health Perspectives 111, 1102-1109.

Wang, C.-Y., Yang, C.-H., Huang, K.-S., Yeh, C.-S., Wang, A.H.-J., Chen, C.-H., 2013. Electrostatic droplets assisted in situ synthesis of superparamagnetic chitosan microparticles for magnetic-responsive controlled drug release and copper ion removal. Journal of Materials Chemistry B 1, 2205-2212.

Wang, H., Wang, H.-L., Jiang, W.-F., Li, Z.-Q., 2009. Photocatalytic degradation of 2, 4-dinitrophenol (DNP) by multi-walled carbon nanotubes (MWCNTs)/TiO_2 composite in aqueous solution under solar irradiation. Water research 43, 204-210.

Wang, P., Huang, B., Dai, Y., Whangbo, M.-H., 2012. Plasmonic photocatalysts: harvesting visible light with noble metal nanoparticles. Physical Chemistry Chemical Physics 14, 9813-9825.

Wang, Z., Zhang, P., Hu, F., Zhao, Y., Zhu, L., 2017. A crosslinked β-cyclodextrin polymer used for rapid removal of a broad-spectrum of organic micropollutants from water. Carbohydrate polymers 177, 224-231.

Xiao, F., Li, W., Fang, L., Wang, D., 2016. Synthesis of akageneite (beta-FeOOH)/reduced graphene oxide nanocomposites for oxidative decomposition of 2-chlorophenol by Fenton-like reaction. Journal of hazardous materials 308, 11-20.

Xie, J., Zhang, L., Li, M., Hao, Y., Lian, Y., Li, Z., Wei, Y., 2015. α-Fe2O3 modified ZnO flower-like microstructures with enhanced photocatalytic performance for pentachlorophenol degradation. Ceramics International 41, 9420-9425.

Xu, C., Liu, R., Chen, L., Tang, J., 2016a. Enhanced dechlorination of 2, 4-dichlorophenol by recoverable Ni/Fe–Fe3O4 nanocomposites. Journal of Environmental Sciences 48, 92-101.

Xu, J., Cao, Z., Liu, X., Zhao, H., Xiao, X., Wu, J., Xu, X., Zhou, J.L., 2016b. Preparation of functionalized Pd/Fe-Fe_3O_4@ MWCNTs nanomaterials for aqueous 2, 4-dichlorophenol removal: Interactions, influence factors, and kinetics. Journal of hazardous materials 317, 656-666.

Xu, X., Zhou, M., He, P., Hao, Z., 2005. Catalytic reduction of chlorinated and recalcitrant compounds in contaminated water. Journal of hazardous materials 123, 89-93.

Yadav, I.C., Devi, N.L., Syed, J.H., Cheng, Z., Li, J., Zhang, G., Jones, K.C., 2015. Current status of persistent organic pesticides residues in air, water, and soil, and their possible effect on neighboring countries: a comprehensive review of India. Science of the Total Environment 511, 123-137.

Yamaguchi, N.U., Bergamasco, R., Hamoudi, S., 2016. Magnetic $MnFe_2O_4$–graphene hybrid composite for efficient removal of glyphosate from water. Chemical Engineering Journal 295, 391-402.

Yang, K.J., Lee, J., Park, H.L., 2020. Organophosphate Pesticide Exposure and Breast Cancer Risk: A Rapid Review of Human, Animal, and Cell-Based Studies. International Journal of Environmental Research and Public Health 17.

Yang, Y., Zhang, Y., Dong, M., Yan, T., Zhang, M., Zeng, Q., 2017. Highly efficient degradation of thidiazuron with Ag/AgCl-activated carbon composites under LED light irradiation. Journal of hazardous materials 335, 92-99.

Yu, H., Wang, X., Sun, H., Huo, M., 2010. Photocatalytic degradation of malathion in aqueous solution using an Au–Pd–TiO_2 nanotube film. Journal of hazardous materials 184, 753-758.

Yu, L., Yang, X., Ye, Y., Wang, D., 2015. Efficient removal of atrazine in water with a Fe_3O_4/MWCNTs nanocomposite as a heterogeneous Fenton-like catalyst. RSC Advances 5, 46059-46066.

Yue, Z., Economy, J., 2005. Nanoparticle and nanoporous carbon adsorbents for removal of trace organic contaminants from water. Journal of Nanoparticle Research 7, 477-487.

Zangeneh, H., Zinatizadeh, A., Habibi, M., Akia, M., Isa, M.H., 2015. Photocatalytic oxidation of organic dyes and pollutants in wastewater using different modified titanium dioxides: A comparative review. Journal of Industrial and Engineering Chemistry 26, 1-36.

Zhang, H., Liang, C., Liu, J., Tian, Z., Wang, G., Cai, W., 2012. Defect-mediated formation of Ag cluster-doped TiO_2 nanoparticles for efficient photodegradation of pentachlorophenol. Langmuir 28, 3938-3944.

Zhao, R., Li, X., Sun, B., Ji, H., Wang, C., 2017. Diethylenetriamine-assisted synthesis of amino-rich hydrothermal carbon-coated electrospun polyacrylonitrile fiber adsorbents for the removal of Cr (VI) and 2, 4-dichlorophenoxyacetic acid. Journal of colloid and interface science 487, 297-309.

Zhao, X., Shi, Y., Cai, Y., Mou, S., 2008. Cetyltrimethylammonium bromide-coated magnetic nanoparticles for the preconcentration of phenolic compounds from environmental water samples. Environmental science & technology 42, 1201-1206.

Zhou, Q., Xiao, J., Wang, W., 2006. Using multi-walled carbon nanotubes as solid phase extraction adsorbents to determine dichlorodiphenyltrichloroethane and its metabolites at trace level in water samples by high performance liquid chromatography with UV detection. Journal of chromatography A 1125, 152-158.

Zhu, X., Li, B., Yang, J., Li, Y., Zhao, W., Shi, J., Gu, J., 2015. Effective adsorption and enhanced removal of organophosphorus pesticides from aqueous solution by Zr-based MOFs of UiO-67. ACS applied materials & interfaces 7, 223-231.

Zhu, X., Yuan, C., Chen, H., 2007. Photocatalytic degradation of pesticide pyridaben. 3. In surfactant/TiO_2 aqueous dispersions. Environmental science & technology 41, 263-269.

List of Tables

Table 1 Role of Ti, Zn, W, Fe based functional materials for removal of the pesticides in aqueous media.

Metal based Functionalized materials	**Contaminants**	**Removal efficacy and Time**	**References**
Titanium based materials			
$AgCl/Ag/TiO_2$	2,4-Dichlorophenol	94.0 %, 60 min	(Tian et al., 2014)
Ag/TiO_2	Pentachlorophenol	100 %, 160 min	(Zhang et al., 2012)
Fe/TiO_2	2,4-Dinitrophenol	97.0 %, 120 min	(Liu et al., 2012)
$Ag/Zr/TiO_2$	4-nitrophenol	100 %, 8 mint	(Naraginti et al., 2015)
$Ag/Cu/TiO_2$	4-nitrophenol	96.0 %, 30 min	(Hernández-Gordillo and González, 2015)
Ti-AC np	Dicofol	97.3%, 89.12 min	(Vali et al., 2021)
Ag/TiO2	Acetamiprid	-, 40 min	(Cao et al., 2008)
$FeFNS/TiO_2$	Diazinon	87.6 %, 100 min	(Hossaini et al., 2014)
TiO_2/Fe_2O_3	Diazinon	95.1 %, 45 min	(Mirmasoomi et al., 2017)
$CTAB\text{-}TiO_2$	Pyridaben	100 %, 560 min	(Zhu et al., 2007)
$TiO_2\text{-}SiO_2$	Dichlorovos,	100 %, 420 min	(Shifu and Gengyu, 2005)
$Fe_2O_3/CuO/TiO_2$	2,4-D	97.0 %, 300 min	(López-Ayala et al., 2015)
Fe/TiO_2	Thiacloprid	96.0 %, 240 min	(Banić et al., 2011)
$Fe_2O3\text{-}TiO_2$	Propachlor	96.0 %, 50 min	(Belessi et al., 2009)
$Au\text{-}Pd\text{-}TiO_2$	Malathion	98.2 %, 240 min	(Yu et al., 2010)
Zinc based materials			
Chitosan-ZnO	Permethrin	99.0 %, 90 min	(Dehaghi et al., 2014)
ZnO-bentonite	Phenol	80.0 %, 90 min	(Meshram et al., 2011)

WO_3-ZnO	Diazinon	99%, 180 min	(Maleki et al., 2020)
rGO-ZnO	Chlorpyrifos	75%, 70 min	(Gulati et al., 2020)
PANI/ZnO-$CoMoO_4$	Imidacloprid	97%, 180 min	(Adabavazeh et al., 2021)
Fe_3O_4/CdS–ZnS	Chlorpyrifos	72%, -	(Soltani-nezhad et al., 2020)
Ag/ZnO	Phosphamidon	100 %, 150 min	(Korake et al., 2012)
ZnO/TiO_2	Diazinon	99.9 %, 60 min	(Jonidi-Jafari et al., 2015)
ZnO/Fe_2O_3	Dicamba	100 %, 300 min	(Maya-Treviño et al., 2014)
Ag/ZnO	4-nitrophenol	100 %, 180 min	(Divband et al., 2013)
Ln/ZnO	4-nitrophenol	83.4 %, 200 min	(Khatamian et al., 2012)
CuO/ZnO	4-nitrophenol	99.0 %, 180 min	(Qamar et al., 2015)
Graphene/ZnO	Nitrophenol	98.0 %, 150 min	(Darwish et al., 2017)
La/ZnO	Metasystox	90.0 %, 150 min	(Korake et al., 2014)
	2,4,6-Trichlorophenol	100 %, 120 min	(Anandan et al., 2007b)
	Monocrotophos	100 %, 120 min	(Anandan et al., 2007a)
Fe_2O3/ZnO	Pentachlorophenol	98.0 %, 240 min	(Xie et al., 2015)
W/ZnO	Chlorophenol	100 %, 150 min	(Aslam et al., 2015)
Sm/ZnO	Phenol	89.5 %, 480 min	(Sin et al., 2013)
Nb_2O_5/ZnO	Phenol	100 %, 40 min	(Lam et al., 2014)
Tungsten based materials			
WO_3	2-Chlorophenol	98.0 %, 180 min	(Aslam et al., 2014)
WO_3-TiO_2	Malathion	99.0 %, 300 min	(Ramos-Delgado et al., 2013)
	Imazapyr	100 %, 120 min	(Ismail et al., 2016)
ZnSe-WO_3	Bisphenol A	99.0 %, 90 min	(Kumar et al., 2017)
Pd-WO_3	2,4-D	100 %, 50 min	(Mkhalid, 2016)
P/W@UiO-66-NH_2 MOFs	4-Nitrophenol	100%, -	(Roshdy et al., 2021)

WO_3/Fe_3O_4	Thiacloprid	91.3%, -	(Banić et al., 2019)
Iron based materials			
$CuFe_3O_4$	4-Nitrophenol	95.0 %, 40s	(Feng et al., 2013)
SDS-coated Fe_3O_4 chitosan NPs	Diazinon	99%	(Ranjbar Bandforuzi and Hadjmohammadi, 2019)
	Phosalone	98%	
	Chlorpyrifos	96%	
Fe/Pd	Lindane	kobs =1.02x0.16 min^{-1} ,5 min	(Nagpal et al., 2010)
Fe_2O_3/MWCNT	Atrazine	81.4 %, 2h	(Yu et al., 2015)
Starched Fe/Pd	Trichloroethylene	98.0 %, 1h	(He and Zhao, 2005)
Ag/iron oxide	Nitrophenol	30 min	(Chiou et al., 2013)
$FeOOH/Fe_2O_3$	Atrazine	95.0 %, 30 min	(Ali et al., 2016)
Ag/Fe microbox	Nitrophenol	kobs = 11.4x102 s^{-1} , 150 min	(Jiang et al., 2015)
$MnFe_2O_4$-graphene	Glyphosate	97.0 %, 8h	(Yamaguchi et al., 2016)
Fe-$ZnIn_2S_4$	Tribromophenol	95.0 %, 60 min	(Gao et al., 2013)
CTAB-Fe_3O_4	Bisphenol A	95.0 %	(Zhao et al., 2008)
$CuFe_2O_4$	Tetrabromobisphenol-A	99.0 %, 30 min	(Ding et al., 2013)
GO-Fe_3O_4	2,4-D	67.2 mg/g	(Nethaji and Sivasamy, 2017)
Fe_3O_4@$nSiO_2$@$mSiO_2$	DDT	97.0 %, 60 min	(Tian et al., 2015)
$CoFe_2O_4$@TiO_2-GO	Chloropyrifos	-, 60 min	(Gupta et al., 2015)
$Ce_xFe_{1-x}O_2$	Chlorophenol, Dichlorophenol, 2,4-D	58.7 %, 90 min, 42.4 %, 90 min, 45.8 %, 60 min	(Kurian et al., 2017)
FeO/activated carbon	Chlordecone	79.8 µg/mg, 1400 min	(Rana et al., 2017)

Pd/Fe–Fe_3O_4@MWCNT	2,4-Dichlorophenol	92.3 %, 300 min	(Xu et al., 2016b)
Fe_3C@N-GE-Fe_3O_4	2,6-dichlorobenzamide (BAM), 2-methyl-4-chlorophenoxy acetic acid (MCPA), 2-methyl-4- chlorophenoxy propionic acid (MCPP)	84%, 93%, 93% respectively	(Ghanbarlou et al., 2020)
Fe turnings	Heptachlor, endosulfan, dieldrin, endrin	5.7, 13.2, 23.3, 39.4% respectively, 10 min	(Abbas et al., 2020)
CaFu MOFs	Imidacloprid	467.23 mg/g	(Singh et al., 2021)
TiO_2@$LaFeO_3$	myclobutanil	100%, 180 min	(Garcia-Muñoz et al., 2020)

1151 **Table 2** Functional polymeric materials for the removal of pesticides.

Functional Group	Material	Target analytes	Experimental conditions	Removal efficacy	Ref
Carbon-based	MWCNT/TiO_2	Dinitrophenol	Dose: 8 g/L, C0: 38 ppm, pH: 6, Sunlight	99%	(Debnath et al., 2019)
	Ti/MWCNT	Atrazine	Dose: 0.2 mg/L C0: 4.6 104 9.3 102 mmol/L	-	(Chen et al., 2011)
	Biochar	Tricyclazole, Isoprothiolane, Malathion	-	63.81, 46.72, 98.08 %	(Tong et al., 2019)
	Silver@graphene oxide	Imidacloprid	-	63%	(Keshvardoostchokami et al., 2018)
	Activated Coconut Charcoal (AcCoC)	monocrotophos	pH 7	103.9 mg/g	(Kodali et al., 2021)
	Plain chitosan	Imidacloprid	pH 6	70%	(Moustafa et al., 2021)
	AgNPs@ chitosan	Imidacloprid	pH 6	95%	(Moustafa et al., 2021)
	Nanoporous activated carbon	Imidacloprid	-	80-99%	(Mohammad and El-Sayed, 2020)
	Ag/AgBr/CNT	Tribromophenol	Dose: 30 mg/50 mL, C0: 100mmol/L pH: 10, 250 W metal halide lamp	100%	(Shi et al., 2013)
	GAC (granular active carbon)	Atrazine, Prometryn, Chlorpyrifos, Dipterex, Acetamiprid, Imidacloprid, Thiamethoxam, Azoxystrobin, Carbendazim, Dimethomorph, Difenoconazole, Prochloraz	-	80, 100, 100, 93.33, 84.95, 100, 72.41, 88.89, 92.80, 83.33, 100, 100 %	(Tang et al., 2020)
	Au/mesoporous carbon	p-Nitrophenol	Dose: 75 mg C0: 200 ppm pH:	87%	(Guo et al., 2016)

			10.1, 0.06 M $NaBH_4$		
	Ag/graphene-dopamine MWCNT-O (0.85%)	4-Nitrophenol Atrazine	$NaBH_4$ Dose: 5 mg/25 mL C0: 4.2 ppm 0.01 M $NaNO_3$ + 0.1 g/L NaN_3, pH: 6	17.3 mg/g	(Chen et al., 2009; Jeon et al., 2013)
	RGO-ZnS RGO-Ag Fe_3O_4/graphene	Nitrophenol Lindane Ametryn	Solar light simulator C0: 2 ppm, Dose: 0.5 g/L, C0: 10 ppm	87% 99% 93.6%	(Boruah et al., 2017; Ibrahim et al., 2017)
	Fe_4O_3–GO–β-cyclodextrin	Thiamethoxam Imidacloprid Acetamiprid Nitenpyram Dinotefuran Clothianidin Thiacloprid	Dose: 5 g/L C0: 10 ppm	2.8 mg/g 3.1 mg/g 2.9 mg/g 2.5 mg/g 2.5 mg/g 1.7 mg/g 2.8 mg/g	(Liu et al., 2017)
	β-FeOOH-RGO	2-Chlorophenol	Dose: 1 g/L C_0: 100 ppm 0.1 M H2O2 pH: 4	100%	(Xiao et al., 2016)
	Ag/AgCl-activated carbon	Thidiazuron	Dose: 0.3 g/L C0: 20 ppm 23 W Philips LED, 20 mW/cm^2 pH: 7	91%	(Yang et al., 2017)
	CoO/TiO_2/GO	Chlorophenol	Dose: 0.5 g/L C0: 10 ppm, 0.01% H_2O_2, 200 W Xenon lamp, pH: 6	97.5%	(Sharma and Lee, 2016)
	Ag/Ag_2CO_3-rGO	Phenol	Dose: 0.05 g/25 mL C0: 10 ppm 350 W Xenon lamp, 40 mW/cm^2	82%	(Song et al., 2016)
	Graphene quantum dot	Oxamyl	Dose: 0.6 g/20 mL C0: 150 ppm pH: 8	125mg/g 95.7%	(Agarwal et al., 2016)
Zirconium	Zirconium-benzene dicarboxylate	Methylchloro-phenoxy propionic	pH: 4, C0: 20 ppm Dose: 0.1 g/L	85%	(Seo et al., 2015)

- based	(UiO-66)	acid			
	Zirconium-benzene dicarboxylate (UiO-67)	Glyphosate	Dose: 0.03 g/L pH: 4, C0: 0.1 mmol/L	537 mg/g	(Zhu et al., 2015)
	UiO-67	Glyphosate	-	540 mg/g	(Pankajakshan et al., 2018)
	NU-1000	Glyphosate	-	1500 mg/g	(Pankajakshan et al., 2018)
	yttria-stabilized ZrO_2 (8YSZ)	Carbofuran	-	89%	(Qin et al., 2020)
	MIL-140A	Nitrophenol	-	91 mg/g	(Lee et al., 2018)
	Zirconium-benzene dicarboxylate (UiO-67)	Glufosinate	Dose: 0.03 g/L pH: 4, C0: 0.1 mmol/L	360 mg/g	(Zhu et al., 2015)
	TiO_2/ZrO_2	Quinalphos	Dose: 4 g/L, pH: 3 C0: 105 M	62%	(Goswami and Ganguli, 2013)
	WO_3/ZrO_3	Carbofuran	Dose: 1 g/L pH: 8, C0: 20 ppm UV flux 50 W/m^2	100%	(Alalm et al., 2016)
	TiO_2/ZrO_2	Chloridazon	Dose: 3 g/L, pH: 8 C0: 5 105 M, 150W Xenon lamp	-	(Mbiri et al., 2018)
Polymer-based	β-Cyclodextrin-chitosan-Fe3O4	Bisphenol A	pH: 6 C0: 200 ppm	133 mg/g	(Huang et al., 2017)
	Polyvinyl-pyridine-co-styrene-montmorillonite clay composite	Diazinon	Dose: 0.5 g/L pH: 3.5 0.13 mM	100%	(Shabtai and Mishael, 2017)
	β-Cyclodextrin	Bisphenol A	Dose: 1 g/L 0.1 mmol/L	113 mg/g	(Wang et al., 2017)
	Carbon coated polyacrylonitrile	2,4-D	Dose: 50 mg/80 mL pH: 3, 70 ppm	61.02 mg/g	(Zhao et al., 2017)
	Montmorillonite-CuO-chitosan	Dichlorovos	Dose: 1.5 g/L pH: 8, 80 ppm	93%	(Sahithya et al., 2015)
	Montmorillonite-CuO- polylactic acid	Monocrotophos	Dose: 15 g/L pH: 5, 100 ppm	80%	(Foo, 2016)

	Starch polymer-laponite clay	Dicamba	Dose: 30 mg/25 mL pH: 7, 500 ppm	251 mg/g	(Pinto et al., 2016)
	Polyaniline-zeolite	Glyphosate	Dose: 50 mg/5 cm3 400 ppm	98.5 mg/g	(Debnath et al., 2019)
	Polyaniline-silica gel	2,6-Dichlorophenol	Dose: 1 g/L pH: 7, 80 ppm	31.9 mg/g	(Pan et al., 2011)
	Polyvinylpyrrolidone-magnetic nanoparticles	Bisphenol-A	pH: 7 50mg/L	90 mg/g	(Fard et al., 2017)
	Bentonite/P.HEMA-MMA	methyl parathion	240 min	868.5 mg/g	(Abukhadra et al., 2021)
	poly (ε-caprolactone)	Endosulfan	30 min	99.97%	(Mourabit and Boulaid, 2019)
	Nano-organoclay composite based on carboxy methyl cellulose and two nano-organobentonites (DMDA, ODAAPS)	Atrazine, butachlor, cabendazim, cabofuran, imidacloprid, isoproturon, pendimethalin, thiophanate methyl, thiamethoxam	-	57.6, 99.6, 66.6, 74.8, 75.3, 96.2, 98.5, 99.9, 76.3%	(Narayanan et al., 2020)

List of Figures

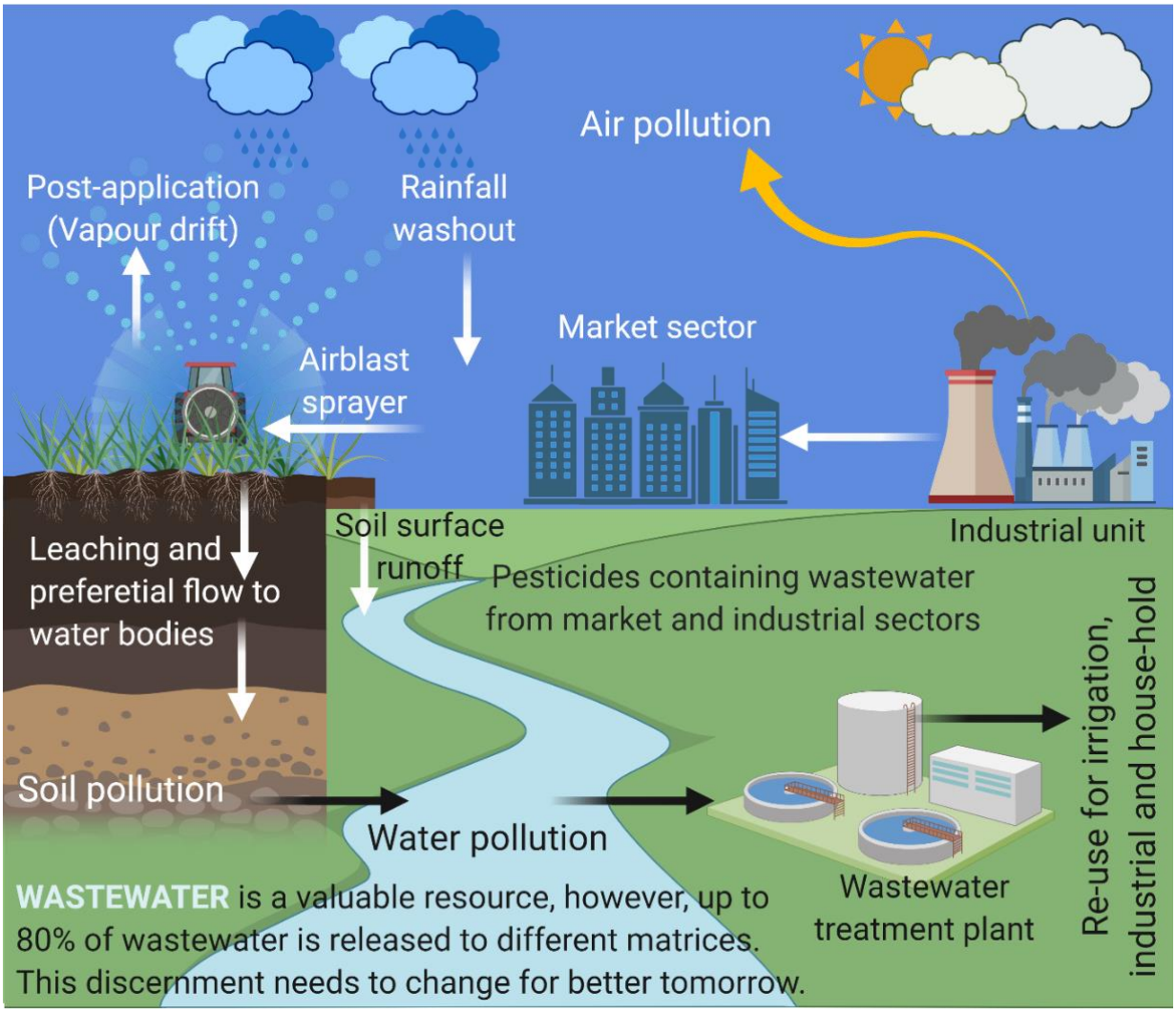

Figure 1 Pesticide drift that can lead to contamination of different environmental matrices including air, soil, and water.

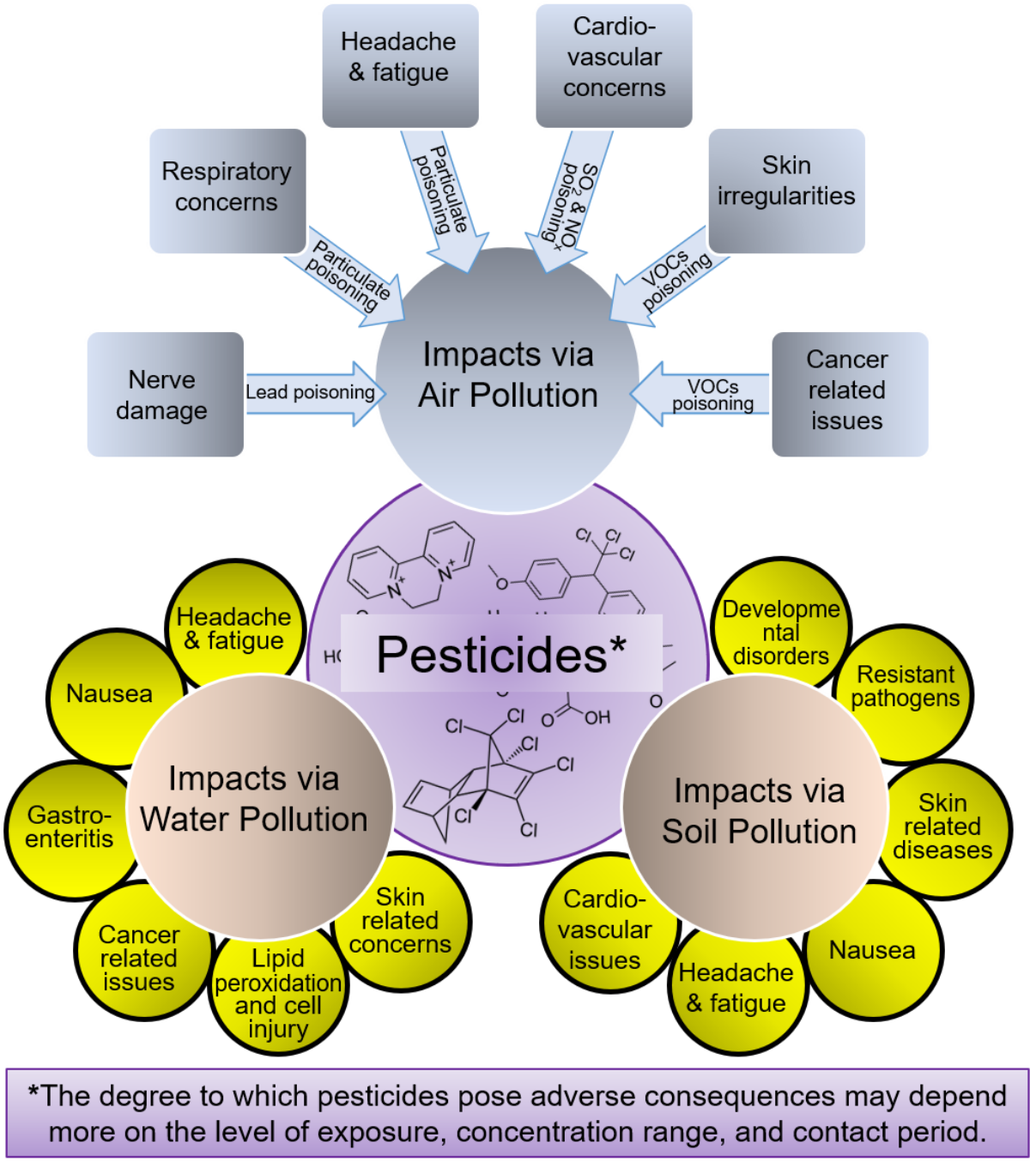

Figure 2 Adverse biological impacts of pesticides via air, water and soil pollution.

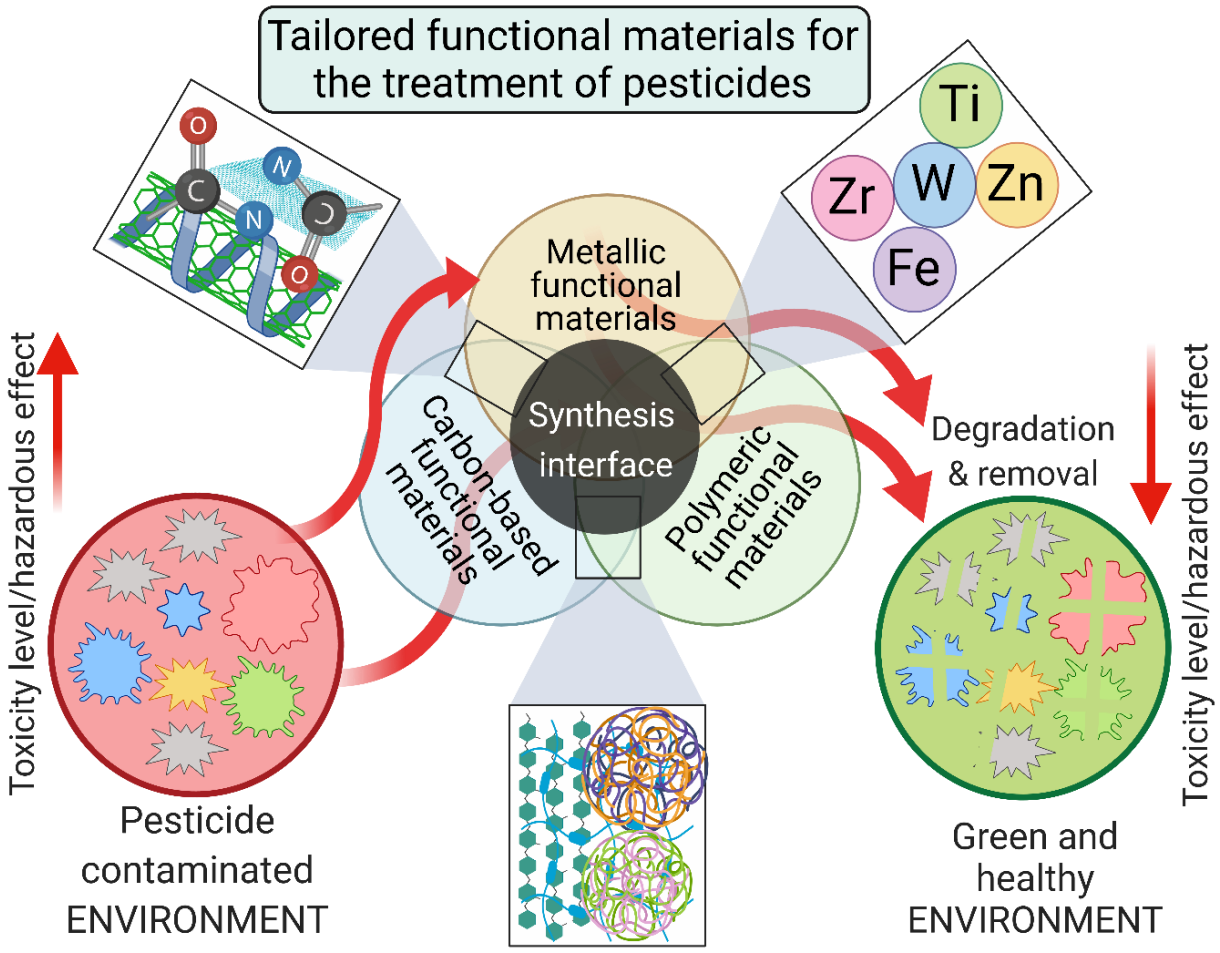

Figure 3 Schematic diagram showing tailored functional materials for the treatment of pesticides and related environmental pollutants.

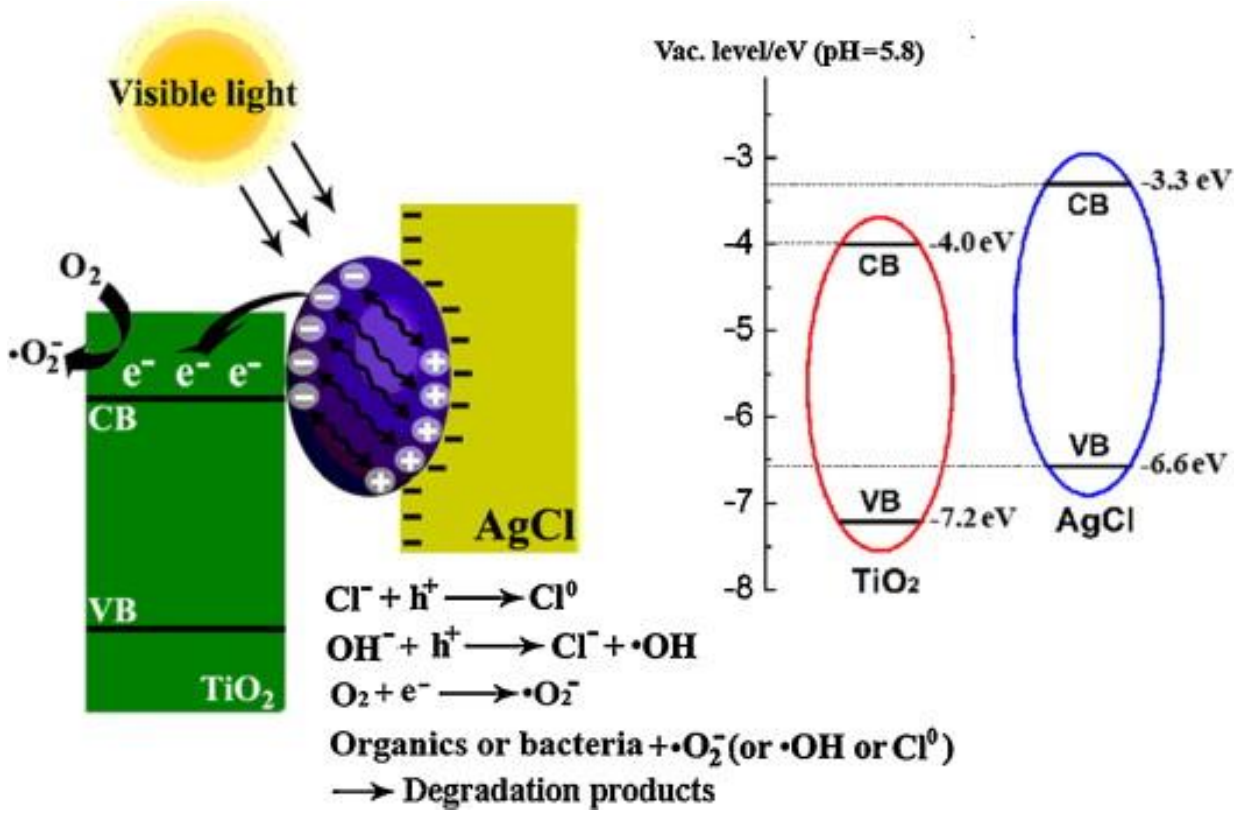

Figure 4 Proposed reaction mechanism of organics (or bacteria) over AgBr@Ag@TiO_2 photocatalyst under visible light irradiation. Reprinted from Tian et al. (2014) with permission from Elsevier. Copyright © 2014 Elsevier B.V. License Number: 5055760857679.

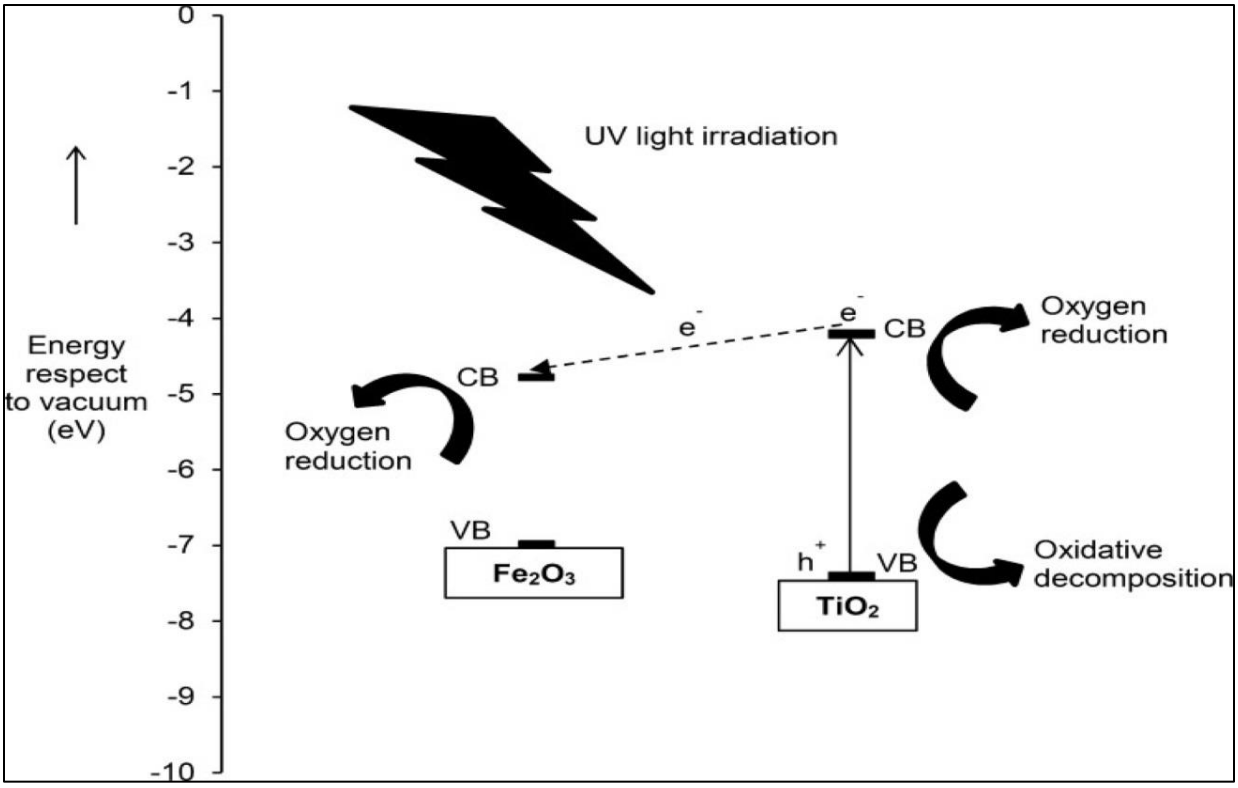

Figure 5 Illustration of the mechanism for major charge transfer pathways on Fe_2O_3(0.5)/TiO_2 (PD) for 2,4-dichlorophenoxyacetic acid degradation. VB stands for valence band and CB stands for conduction band. Reprinted from Lee et al. (2017) with permission under the terms of the Creative Commons Attribution License.

(http://creativecommons.org/licenses/by/4.0).

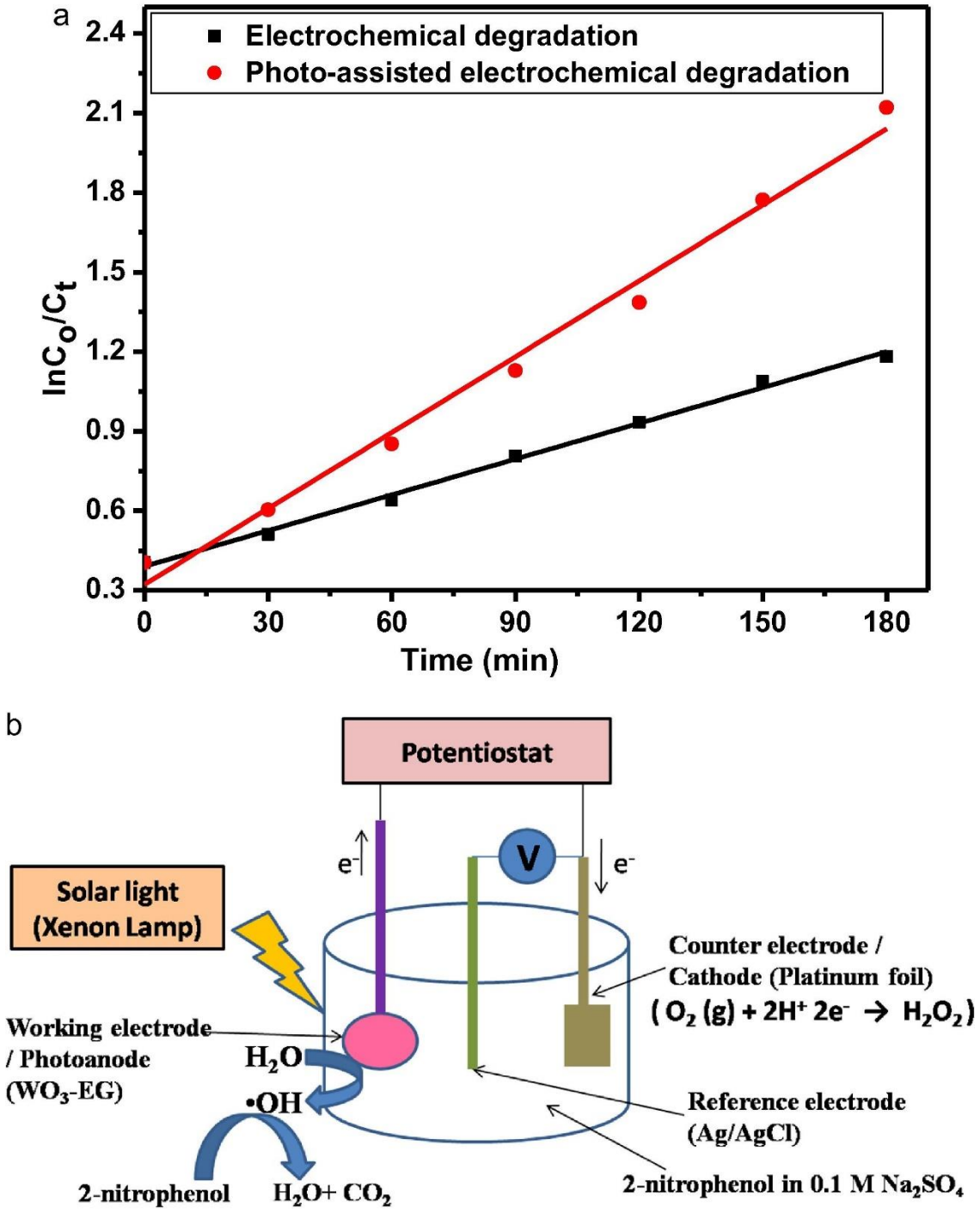

Figure 6 (a) Degradation kinetics graphs of electrochemical and photo-assisted electrochemical degradation of 2-nitrophenol dye at pH 6 and 10 mA cm^{-2} using WO_3-EG composite electrode; (b) Proposed underlying charge transfer mechanism of the photo-assisted activity of WO_3-EG composite electrode for the degradation of 2-nitrophenol. Reprinted from Umukoro et al. (2017) with permission from Elsevier. Copyright © 2017 Elsevier B.V. License Number: 5055761305400.

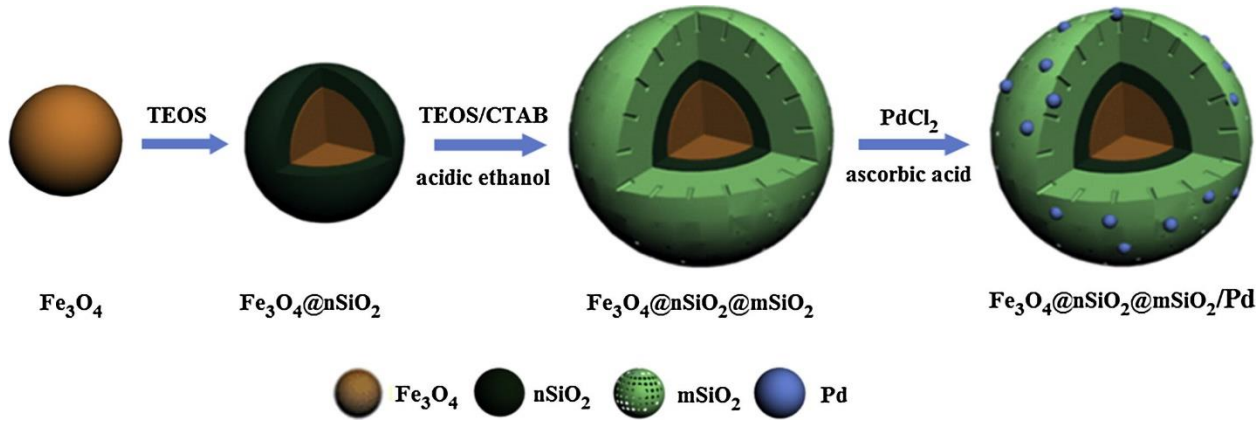

Figure 7 Schematic of $Fe_3O_4/nSiO_2/mSiO_2/Pd$ formation. Reprinted from Tian et al. (2015) with permission from Elsevier. Copyright © 2015 Elsevier Inc. License Number: 5055770011546.